

MCMC Importance Sampling via Moreau-Yosida Envelopes

Apratim Shukla
 Dept. of Mathematics and Statistics
 IIT Kanpur
 apratims21@iitk.ac.in

Dootika Vats
 Dept. of Mathematics and Statistics
 IIT Kanpur
 dootika@iitk.ac.in

Eric C. Chi
 Department of Statistics
 Rice University
 echi@rice.edu

January 7, 2025

Abstract

The use of non-differentiable priors is standard in modern parsimonious Bayesian models. Lack of differentiability, however, precludes gradient-based Markov chain Monte Carlo (MCMC) methods for posterior sampling. Recently proposed proximal MCMC approaches can partially remedy this limitation. These approaches use gradients of a smooth approximation, constructed via Moreau-Yosida (MY) envelopes, to make proposals. In this work, we build an importance sampling paradigm by using the MY envelope as an importance distribution. Leveraging properties of the envelope, we establish asymptotic normality of the importance sampling estimator with an explicit expression for the asymptotic covariance matrix. Since the MY envelope density is smooth, it is amenable to gradient-based samplers. We provide sufficient conditions for geometric ergodicity of Metropolis-adjusted Langevin and Hamiltonian Monte Carlo algorithms, sampling from this importance distribution. A variety of numerical studies show that the proposed scheme can yield lower variance estimators compared to existing proximal MCMC alternatives, and is effective in both low and high dimensions.

1 Introduction

Markov chain Monte Carlo (MCMC) is a popular algorithm for sampling from complex and high-dimensional distributions. For a function $\psi : \mathbb{R}^d \rightarrow (-\infty, \infty]$, we consider the

problem of estimating characteristics of a target density of the form

$$\pi(x) \propto e^{-\psi(x)}. \quad (1)$$

Such potentially intractable densities arise in numerous areas, but most noticeably appear as posterior distributions in Bayesian statistics. MCMC enables the estimation of features of π by constructing a Markov chain with π as its stationary and limiting distribution. The complexity of modern data has led to increasingly sophisticated models across various applications, and sampling from the resulting posteriors can be challenging. Consequently, much work in MCMC has gone into constructing effective sampling and estimation strategies that are locally informed, utilizing the geometry of the posterior density to inform the next move of the Markov chain.

Gradient-based MCMC algorithms account for the local geometry of π by utilizing $\nabla\psi(x)$ in the proposal distribution within the popular Metropolis-Hastings sampler. These methods include the Metropolis-Adjusted Langevin Algorithm (MALA) (Roberts and Rosenthal, 1998), Hamiltonian Monte Carlo (HMC) (Neal et al., 2011), Riemannian manifold MALA and HMC (Girolami and Calderhead, 2011), and Barker’s proposals (Livingstone and Zanella, 2022). Gradient-based MCMC algorithms can converge faster to the target distribution (Beskos et al., 2013; Roberts and Rosenthal, 1998; Vogrinc et al., 2023) than uninformed algorithms like random walk Metropolis.

Chief among the requirements to implement gradient-based algorithms, is the differentiability of ψ . Non-differentiable priors that induce structured sparsity in model parameters are often used for modern data. Effective sampling and estimation from the resulting non-differentiable posteriors is a challenge, since it precludes a straightforward use of gradient-based MCMC methods. Major progress, however, in removing the barrier to using gradient-based MCMC methods for non-smooth target densities came in Pereyra

(2016). This work introduced a MALA-like MCMC algorithm, called proximal MALA, for sampling from a non-smooth target density, π . The key idea is to replace gradients of ψ in the MALA proposal with gradients of its Moreau-Yosida envelope, ψ^λ . The Moreau-Yosida envelope ψ^λ is Lipschitz differentiable. Thus, the gradient of ψ^λ not only exists but is also well-behaved. Nonetheless, although it is relatively effective, the algorithm can suffer from slow convergence thus yielding high variance estimators of posterior quantities (Durmus et al., 2022). A primary reason of slow convergence is that the gradient of the approximation ψ^λ may not adequately capture the geometry of ψ . Fortunately, in importance sampling, there is a natural strategy for variance reduction for exactly these situations.

Importance sampling is a classic approach of using samples generated from a proxy distribution, called the importance distribution, to estimate characteristics of a target distribution. If the importance distribution is chosen well, the variance of the importance sampling estimator can be orders of magnitude smaller than the variance of the estimator computed with samples from π . Conversely, if the importance distribution is chosen poorly, estimators can have larger variance – even infinite variance. The success and failure of importance sampling hinges critically on the choice of the importance distribution.

We propose a simple and general way to design effective importance distributions for a given π that either suffers from non-differentiability or lack of gradient Lipschitzness. Specifically, we use the Moreau-Yosida envelope, ψ^λ , to approximate the function ψ and implement importance sampling with the importance density $\pi^\lambda(x) \propto e^{-\psi^\lambda(x)}$. Since π^λ possesses well-behaved gradients, gradient-based MCMC samplers like MALA and HMC can effectively sample from π^λ . We present importance sampling estimators for expectations under π . Our estimators are guaranteed to have finite asymptotic variance. We also present practical ways to estimate this asymptotic variance for both univariate and multivariate expectations. Acknowledging that credible intervals are an integral part of the

Bayesian workflow, we also provide importance sampling estimators of marginal quantiles.

Finiteness of the asymptotic variance of importance sampling estimators naturally requires the underlying Markov chains to converge at a fast enough rate. For MALA and HMC chains, invariant for π^λ , we present sufficient conditions for geometric ergodicity. Specifically, we identify situations when MALA or HMC would not be geometrically ergodic for π but are geometrically ergodic for the corresponding π^λ .

The rest of the paper is organized as follows. Section 2 briefly reviews importance sampling schemes and Section 3 reviews the Moreau-Yosida envelope, the proximal operator, and the proximal MCMC algorithms based on them. Section 4 introduces our proposed sampling scheme and estimator, discusses the estimation of means and quantiles, and presents critical theoretical results and practical considerations. Section 5 takes a closer look at the MALA and HMC algorithms targeting the Moreau-Yosida envelope π^λ and presents results under which these algorithms are geometrically ergodic. In Section 6 we present numerical studies illustrating the utility of our proposed strategy over existing alternatives. In addition to toy examples with simple target densities, we implement our proposed strategy on a Bayesian trendfiltering problem, an image denoising via low rank matrix estimation problem, and for a Bayesian Poisson random effects model. Section 7 ends with a discussion. All proofs and some details on the examples are provided in the Appendix.

2 Importance sampling

Consider a distribution with density π defined on \mathbb{R}^d , of the form in (1) and a function $\xi : \mathbb{R}^d \rightarrow \mathbb{R}^p$. A fundamental task is to estimate

$$\theta := \mathbb{E}_\pi[\xi(X)] = \int_{\mathbb{R}^d} \xi(x)\pi(x)dx < \infty. \quad (2)$$

We use the notation \mathbb{E}_π to indicate that the expectation is with respect to a distribution with density π . Importance sampling methods estimate θ using weighted samples from an importance distribution with density g , whose support contains the support of π . The key idea is to express an expectation with respect to π , as an expectation with respect to g ,

$$\theta = \int_{\mathbb{R}^d} \xi(x)\pi(x)dx = \int_{\mathbb{R}^d} \xi(x)\frac{\pi(x)}{g(x)}g(x)dx = \mathbb{E}_g \left[\xi(X)\frac{\pi(X)}{g(X)} \right]. \quad (3)$$

First introduced in statistics by Kloek and Van Dijk (1978), importance sampling has most significantly been used when independent and identically distributed (iid) samples from g can be obtained.

When iid samples from g are difficult to obtain but it is easy to simulate a Markov chain $\{X_t\}_{t \geq 1}$ that has g as its stationary and limiting density, a natural strategy to estimate θ in light of (3), is to use

$$\tilde{\theta}_n^g := \frac{1}{n} \sum_{t=1}^n \xi(X_t) \frac{\pi(X_t)}{g(X_t)}. \quad (4)$$

When either π or g is known only up to a normalizing constant, $\tilde{\theta}_n^g$ in (4) cannot be computed. Fortunately, one can introduce a rescaling that eliminates the need for normalization constants. For $g(x) \propto \tilde{g}(x)$, let $w(x) = \exp(-\psi(x))/\tilde{g}(x)$. The self-normalized importance sampling estimator of θ from g is

$$\hat{\theta}_n^g = \sum_{t=1}^n \frac{\xi(X_t)w(X_t)}{\sum_{k=1}^n w(X_k)}. \quad (5)$$

When the Markov chain $\{X_t\}_{t \geq 1}$ is g -ergodic, $\hat{\theta}_n^g$ is strongly consistent¹.

Theorem 1. Let $\{X_t\}_{t \geq 1}$ be an irreducible, aperiodic, and Harris recurrent Markov chain

¹Theorem 1 is generally known, but we have not been able to find a reference, so we present the proof in Appendix A for completeness.

with stationary density g . Then, as $n \rightarrow \infty$, $\hat{\theta}_n^g \xrightarrow{\text{a.s.}} \theta$.

As a consequence of (5), Tierney (1994) highlighted that MCMC samples from the importance distribution can just as well be used in importance sampling, and this strategy has been employed with some success. Silva and Zanella (2023) used MCMC importance samples for implementing Bayesian leave-one-out cross-validation, Madras and Piccioni (1999) obtained a univariate theoretical paradigm for problems in statistical physics, Schuster and Klebanov (2020) used importance sampling inspired weighted averaging to remove bias from the unadjusted Langevin algorithm, and Buta and Doss (2011); Tan et al. (2015) used MCMC importance sampling with multiple Markov chains for applications in Bayesian sensitivity analysis. However, many of these examples are either low-dimensional or quite specific for cases when natural choices of g are easily available.

Successful implementation of importance sampling is possible when (i) it is easier to construct faster converging g -invariant Markov kernels than π -invariant kernels and (ii) when the tails of g can adequately bound $\xi(x)\pi(x)$ to ensure low variance of $\hat{\theta}_n^g$. In fact, if g is chosen well, the variance of $\hat{\theta}_n^g$ can be order of magnitudes lower than the variance of standard Monte Carlo. On the other hand, finiteness of the second moment of ξ under π does not guarantee a finite variance of $\hat{\theta}_n^g$. Thus, if g is not carefully chosen, the estimator $\hat{\theta}_n^g$ can be catastrophically worse than the standard Monte Carlo estimator. Consequently, the importance density g plays a critical role in the quality of $\hat{\theta}_n^g$, but there is little general guidance on how to choose g in practice. For the iid case, this difficult situation is well summarized by a result in Hesterberg (1988, Chapter 2.9) which provides the optimal choice of g as

$$g^*(x) \propto |\xi(x) - \theta|\pi(x). \quad (6)$$

Unfortunately, g^* is not useful in practice since it requires the knowledge of θ , the quantity we are trying to estimate, as well as a means for drawing samples from a distribution with density g^* .

The main contribution of this paper is a general strategy for constructing an effective g for a log-concave π that leads to an estimator $\hat{\theta}_n^g$ with finite asymptotic variance. We focus on target distributions π when ψ 's proximal mapping can be computed efficiently. This enables the construction of a practical importance distribution using a smooth approximation of π via the Moreau-Yosida envelope of ψ . Our proposed importance distribution is guaranteed to yield finite variance estimators. Moreover, the degree of smoothness in the importance distribution can be tuned to yield estimators with smaller variance than usual MCMC estimators. While our primary focus when we started this work was on log-concave π that are not smooth, our approach also applies to differentiable log-concave π for which popular algorithms like MALA and HMC are ineffective. This is particularly true when ψ is not Lipschitz differentiable. In these cases, our Moreau-Yosida importance distributions yield gradients that are Lipschitz facilitating the movement of the Markov chains.

3 Proximal Markov chain Monte Carlo

3.1 Moreau-Yosida envelopes and proximal maps

We review relevant concepts from convex analysis, specifically Moreau-Yosida envelopes and proximal mappings. For a more thorough review of proximal mappings and their applications in statistics and machine learning, we refer readers to Combettes and Wajs (2005); Combettes and Pesquet (2011); Polson et al. (2015).

Let $\Gamma(\mathbb{R}^d)$ denote the set of all proper, lower-semicontinuous, convex functions from \mathbb{R}^d into $\mathbb{R} \cup \{\infty\}$. We restrict our attention to targets π such that $\psi \in \Gamma(\mathbb{R}^d)$. Let $\|\cdot\|$ denote

the Euclidean norm.

Definition 1. Given a positive scaling parameter λ , the *Moreau-Yosida envelope* of $\psi \in \Gamma(\mathbb{R}^d)$ is given by

$$\psi^\lambda(x) = \inf_{y \in \mathbb{R}^d} \left\{ \psi(y) + \frac{1}{2\lambda} \|y - x\|^2 \right\}. \quad (7)$$

The infimum in (7) is always attained at a unique point because $\psi \in \Gamma(\mathbb{R}^d)$. The unique minimizer of (7) defines the proximal mapping of ψ .

Definition 2. Given a positive scaling parameter λ , the *proximal mapping* of $\psi \in \Gamma(\mathbb{R}^d)$ is the operator

$$\text{prox}_\psi^\lambda(x) = \arg \min_{y \in \mathbb{R}^d} \left\{ \psi(y) + \frac{1}{2\lambda} \|y - x\|^2 \right\}. \quad (8)$$

The function $\psi^\lambda(x)$ is called the Moreau-Yosida envelope of $\psi(x)$ because for all $\lambda > 0$ and $x \in \mathbb{R}^d$,

$$\psi^\lambda(x) = \psi(\text{prox}_\psi^\lambda(x)) + \frac{1}{2\lambda} \|\text{prox}_\psi^\lambda(x) - x\|^2 \leq \psi(x), \quad (9)$$

where the last inequality follows from the definition of $\text{prox}_\psi^\lambda(x)$. Therefore, $\psi^\lambda(x)$ “envelopes” $\psi(x)$ from below.

To illustrate these concepts concretely, consider $\pi(x) \propto e^{-|x|}$, so $\psi(x) = |x|$. Its Moreau-Yosida envelope is the Huber function

$$\psi^\lambda(x) = \begin{cases} \frac{1}{2\lambda} x^2 & \text{if } |x| \leq \lambda \\ |x| - \frac{\lambda}{2} & \text{otherwise.} \end{cases}$$

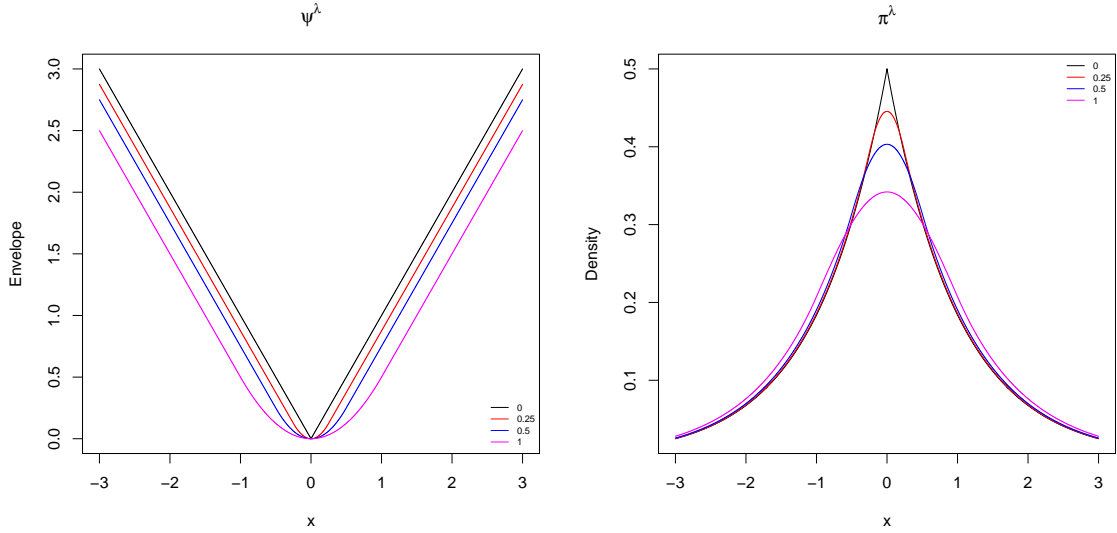


Figure 1: (Left) Moreau-Yosida envelope for $\psi(x) = |x|$ for different values of λ . (Right) The corresponding envelopes for the Laplace distribution.

The left panel of Figure 1 shows $\psi(x)$ and $\psi^\lambda(x)$ for three different λ values. We see that the Moreau-Yosida envelope provides a differentiable approximation to a non-smooth function where the approximation improves as λ gets smaller.

Having constructed ψ^λ , consider the importance density

$$\pi^\lambda(x) \propto e^{-\psi^\lambda(x)}, \quad (10)$$

that is integrable over \mathbb{R}^d for all $\lambda > 0$ (Durmus et al., 2022). The right panel of Figure 1 shows the densities π^λ corresponding to the Moreau-Yosida envelope, ψ^λ .

Proposition 1. [Durmus et al. (2022); Pereyra (2016)] Let $\psi \in \Gamma(\mathbb{R}^d)$ be bounded from below. Then the following hold.

- (a) The function π^λ in (10) defines a proper density of a probability measure on \mathbb{R}^d , i.e., $\int_{\mathbb{R}^d} e^{-\psi^\lambda(x)} dx < \infty$.

- (b) The importance density $\pi^\lambda(x)$ converges to $\pi(x)$ pointwise as $\lambda \rightarrow 0$.
- (c) The importance density $\pi^\lambda(x)$ is continuously differentiable even if π is not. Moreover,

$$\nabla \log \pi^\lambda(x) = \frac{1}{\lambda} \left(\text{prox}_\psi^\lambda(x) - x \right).$$

- (d) A point $x^* \in \mathbb{R}^d$ maximizes π if and only if x^* maximizes π^λ .

The results in Proposition 1 are critical to building an effective importance sampling paradigm using Moreau-Yosida envelopes.

3.2 Proximal and Moreau-Yosida MCMC algorithms

Langevin algorithms like MALA, built from a discretization of the continuous-time Langevin diffusion, are ubiquitous in modern day MCMC applications and are well studied (Roberts and Rosenthal, 2001; Roberts and Tweedie, 1996). Langevin algorithms require the existence of the gradients of $\log \pi(x)$ and that the gradient itself cannot grow larger than $\|x\|$. Specifically, Roberts and Tweedie (1996) show that for bounded π , the MALA algorithm fails to be geometrically ergodic if

$$\liminf_{\|x\| \rightarrow \infty} \frac{\|\nabla \log \pi(x)\|}{\|x\|} > c, \tag{11}$$

where the expression for c is known. Geometric ergodicity is a sufficient condition for the existence of a Markov chain central limit theorem for ergodic averages and thus controls the overall accuracy of the results.

Recently Pereyra (2016) and Durmus et al. (2022) extend Langevin algorithms to generate samples from non-smooth target densities. Given a target density of the form (1), the proximal MALA (P-MALA) algorithm of Pereyra (2016) and the Moreau-Yosida un-

adjusted Langevin algorithm (MY-ULA) of Durmus et al. (2022) employ a discretization of the Langevin diffusion for π^λ , to yield a candidate y from a given x :

$$y = x + \frac{h}{2} \nabla \log \pi^\lambda(x) + \sqrt{h}Z, \quad (12)$$

where $Z \sim N(0, \mathbb{I}_d)$ and $h > 0$ is a step size. Pereyra (2016) uses y as a proposal in a Metropolis-Hastings step ensuring π -invariance, and Durmus et al. (2022) accept y as the next state of the chain, without an accept-reject step. MY-ULA is inexact due to both the discretization error and the discrepancy between π and π^λ . P-MALA is an exact algorithm that yields a π -invariant Markov chain, with scaling fixed as $h = 2\lambda$. As we will see in Section 6, however, P-MALA can often suffer from inefficient estimation compared to our proposed solution explained in the sequel.

Hamiltonian Monte Carlo (HMC) is another popular gradient-based MCMC algorithm. Chaari et al. (2016) construct a modified HMC proposal aimed at efficient sampling from non-smooth densities. They define the HMC proposal based on proximal mappings utilizing gradients of ψ^λ instead of gradients of ψ . In our examples, we also compare our proposed method to this proximal mapping based HMC (P-HMC) algorithm of Chaari et al. (2016).

4 Moreau-Yosida importance sampling

4.1 Moreau-Yosida importance sampling estimator

We propose employing π^λ as an importance density to estimate expectations and quantiles under π . Let $\{X_t\}_{t \geq 1}$ be an irreducible, aperiodic, and Harris recurrent Markov chain with stationary density π^λ . Using notation from Section 2, define the unnormalized weights as

$$w^\lambda(x) = \frac{e^{-\psi(x)}}{e^{-\psi^\lambda(x)}} = e^{-\{\psi(x) - \psi^\lambda(x)\}}. \quad (13)$$

The importance sampling estimator of θ corrects for the mismatch between π and π^λ by utilising a weighted average of the MCMC samples. We denote the *Moreau-Yosida importance sampling (MY-IS)* estimator as,

$$\hat{\theta}_n^{\text{MY}} = \sum_{t=1}^n \frac{\xi(X_t)w^\lambda(X_t)}{\sum_{k=1}^n w^\lambda(X_k)}. \quad (14)$$

Computing $\hat{\theta}_n^{\text{MY}}$ is straightforward. At each iteration we just need to evaluate ξ and w^λ at the current Markov chain state X_t and update a running sum of weights.

Remark 1. As discussed in Pereyra (2016) and Durmus et al. (2022), proximal MCMC methods require the evaluation of ψ^λ in (7). Computing a proximal map may require solving an optimization problem. In many cases the problem does not admit a closed form solution and requires an iterative solver. In these cases, ψ^λ can only be evaluated up to an ϵ tolerance, yielding ψ_ϵ^λ . Despite the numerical approximation, however, the consistency of the importance sampling estimator remains valid, since the weights also change to $w_\epsilon^\lambda(x) = e^{-\{\psi(x) - \psi_\epsilon^\lambda(x)\}}$.

A universal challenge in importance sampling is ensuring the finiteness of the variance of the importance sampling estimator. The following condition on the weights ensures finite variance of an importance sampling estimator,

$$\sup_{x \in \mathbb{R}^d} w(x) < \infty. \quad (15)$$

Under (15) finite variance is guaranteed when $\{X_t\}_{t \geq 1}$ are iid. Madras and Piccioni (1999) present efficient conditions for when $\{X_t\}_{t \geq 1}$ is a univariate Markov chain.

The unnormalized weights $w^\lambda(x)$ satisfy (15) because of the global underestimation bound in (9). We show that (15) is also sufficient to obtain asymptotic normality of $\hat{\theta}_n^{\text{MY}}$ provided the π^λ -invariant Markov chain converges at a geometric rate.

Theorem 2. Let $\{X_t\}_{t \geq 1}$ be a π^λ -reversible, geometrically ergodic Markov chain. If $\mathbb{E}_\pi \|\xi(X_1)\|^2 < \infty$, then as $n \rightarrow \infty$

$$\sqrt{n} \left(\hat{\theta}_n^{\text{MY}} - \theta \right) \xrightarrow{d} N_p(0, \Xi),$$

where

$$\Xi = \frac{1}{[\mathbb{E}_{\pi^\lambda}(w^\lambda(X_1))]^2} \begin{bmatrix} \mathbf{I}_p & -\theta \end{bmatrix} \Sigma \begin{bmatrix} \mathbf{I}_p \\ -\theta^\top \end{bmatrix}, \quad (16)$$

and

$$\begin{aligned} \Sigma &= \text{Var}_{\pi^\lambda} S(X_1) + \sum_{k=1}^{\infty} \text{Cov}_{\pi^\lambda}(S(X_1), S(X_{1+k})) + \sum_{k=1}^{\infty} \text{Cov}_{\pi^\lambda}(S(X_{1+k}), S(X_1)), \\ S(x) &= \begin{pmatrix} \xi(x)w^\lambda(x) \\ w^\lambda(x) \end{pmatrix}. \end{aligned} \quad (17)$$

Proof. See Appendix B. □

Remark 2. For simplicity, we only present one set of sufficient conditions under which asymptotic normality holds, focusing on reversible Markov chains. Using the results of Jones (2004), sufficient conditions can also be obtained when the π^λ -Markov chain is non-reversible, uniformly ergodic, or polynomially ergodic.

The utility of Theorem 2 is three-fold: (i) it guarantees that all choices of λ yield a finite variance estimator, (ii) moment conditions are under π and not the relatively unstudied π^λ , and (iii) the expression of the limiting variance Ξ is explicit. In Section 4.2 we provide estimators of Ξ which enable practitioners to assess simulation quality and

determine whether sufficiently many Monte Carlo samples have been obtained. See Agarwal et al. (2022); Glynn and Whitt (1991); Roy (2019); Vats et al. (2019).

Theorem 2 requires the Markov chain employed for π^λ to be reversible and geometrically ergodic. In our examples, we focus on the MALA and the HMC algorithms, and in Section 5 we present sufficient conditions for these algorithms to be geometrically ergodic. Algorithm 1 presents the π^λ -MALA algorithm, and Algorithm 2 presents the π^λ -HMC algorithm.

Algorithm 1 π^λ -MALA given $h > 0$

1. Given $X_t = x$, generate $Y = y$ from $N\left(x - \frac{h}{2}\nabla\psi^\lambda(x), h\mathbb{I}_d\right)$ with density $q_M(x, \cdot)$
2. Generate $U \sim U(0, 1)$ independently and set

$$\alpha(x, y) = \min\left\{1, \frac{\pi^\lambda(y)q_M(y, x)}{\pi^\lambda(x)q_M(x, y)}\right\}$$

3. If $U \leq \alpha(x, y)$, then $X_{t+1} = y$
 4. Else $X_{t+1} = x$
-

4.2 Estimation of asymptotic variance

Theorem 2 guarantees that, subject to convergence rates of the π^λ -Markov chain, the MY-IS estimator has a finite covariance matrix Ξ . Practitioners would further require an estimator of Ξ in order to assess the Monte Carlo error in estimation. This involves estimating Σ in (17), the asymptotic covariance matrix in the Markov chain central limit theorem for the process $\{S(X_t)\}_{t \geq 1}$. A number of estimators of the asymptotic covariance are available in the literature. Chen and Seila (1987) and Vats et al. (2019) employ a batch means estimator and demonstrate its strong consistency. We employ this estimator due to

Algorithm 2 π^λ -HMC given $\varepsilon > 0$, $L \geq 1$ and $M_{d \times d} \succ 0$

1. Given $X_t = x_0$, draw $z_0 \sim N(0, M)$
2. Use the *leapfrog* one- ε step equations,

$$\begin{aligned} z_{\frac{\varepsilon}{2}} &= z_0 - \frac{\varepsilon}{2} \nabla \psi^\lambda(x_0) \\ x_\varepsilon &= x_0 + \varepsilon M^{-1} z_{\frac{\varepsilon}{2}} \\ z_\varepsilon &= z_{\frac{\varepsilon}{2}} - \frac{\varepsilon}{2} \nabla \psi^\lambda(x_\varepsilon) \end{aligned}$$

L times sequentially to reach $(x_0, z_0) \rightarrow (x_{L\varepsilon}, z_{L\varepsilon})$

3. Draw $U \sim U(0, 1)$ independently, and calculate

$$\alpha(x_0, x_{L\varepsilon}) = \min \left\{ 1, e^{-H(x_{L\varepsilon}, z_{L\varepsilon}) + H(x_0, z_0)} \right\},$$

where $H(x, z) = \psi^\lambda(x) + \frac{1}{2} z^\top M^{-1} z$ denotes total energy at (x, z)

4. If $U \leq \alpha(x_0, x_{L\varepsilon})$, then $X_{t+1} = x_{L\varepsilon}$
 5. Else $X_{t+1} = x_0$
-

its computational efficiency and well established asymptotic properties.

Let $n = ab$ where a denotes the number of batches and b , the size of a batch. Let $\bar{T}_k = b^{-1} \sum_{j=1}^b S(X_{kb+j})$ for $k = 0, 1, \dots, a-1$ be the mean vector of the k^{th} batch, and $\bar{S}_n = n^{-1} \sum_{t=1}^n S(X_t)$ be the overall mean. The batch means estimator of Σ is defined as

$$\hat{\Sigma}_n = \frac{b}{a-1} \sum_{k=0}^{a-1} (\bar{T}_k - \bar{S}_n)(\bar{T}_k - \bar{S}_n)^\top.$$

Using $\hat{\Sigma}_n$, a plug-in estimator of Ξ can be constructed. Denote

$$\bar{w}_n = \frac{1}{n} \sum_{t=1}^n w^\lambda(X_t).$$

Then a plug-in estimator of Ξ is

$$\hat{\Xi}_n^{\text{BM}} = \frac{1}{\bar{w}_n^2} \begin{bmatrix} \mathbf{I}_p & -\hat{\theta}_n^{\text{MY}} \end{bmatrix} \hat{\Sigma}_n \begin{bmatrix} \mathbf{I}_p \\ -(\hat{\theta}_n^{\text{MY}})^\top \end{bmatrix}. \quad (18)$$

Under the strong consistency conditions for $\hat{\Sigma}_n$ discussed in Vats and Flegal (2022); Vats et al. (2019) and using the continuous mapping theorem, $\hat{\Xi}_n^{\text{BM}}$ can also be shown to be strongly consistent. Alternative estimators of Σ exist that may better suit a user's preferences. Spectral variance estimators (Vats et al., 2018), regenerative estimators (Seila, 1982), moment least squares estimators (Berg and Song, 2023; Song and Berg, 2024), and initial sequence estimators (Banerjee and Vats, 2024; Dai and Jones, 2017; Geyer, 1992) are all well-studied with conditions for strong consistency available. See Flegal and Kurtz-Garcia (2024) for a detailed review. We thus present the following result generally for any estimator of Σ .

Theorem 3. Let $\hat{\Sigma}$ be strongly consistent for Σ , and let $\hat{\Xi}_n$ be the estimator of Ξ constructed using $\hat{\Sigma}$. Then, $\hat{\Xi}_n \xrightarrow{\text{a.s.}} \Xi$ as $n \rightarrow \infty$.

Proof. The result follows from the continuous mapping theorem and the fact that both $\hat{\theta}_n^{\text{MY}}$ and \bar{w}_n are strongly consistent. \square

4.3 Quantile estimation

Credible intervals are critical for a complete Bayesian analysis. Glynn et al. (1996) present importance sampling quantiles and establish fundamental theoretical guarantees when π is one-dimensional. Since Bayesian application areas are typically high-dimensional, their methodology does not apply directly. We instead employ the importance sampling quantile estimation procedure proposed by Chen and Shao (1999). The methodology holds in general for a MCMC based importance sampling scheme.

Let the target and importance densities be defined as in (1) and (10). For a vector $x \in \mathbb{R}^d$, let x_i denote its i^{th} component, for $i = 1, 2, \dots, d$. Further, let π_i denote the i^{th} marginal density of π and let Π_i denote its cumulative distribution function. The α^{th} marginal quantile for component i is given as,

$$x_i^{(\alpha)} = \inf \{y \in \mathbb{R} : \Pi_i(y) \geq \alpha\}.$$

Let $\mathbb{1}_{\mathcal{A}_s}(\cdot)$ denote the indicator function on the set $\mathcal{A}_s = \{t \in \mathbb{R} : t \leq s\}$. Then

$$\Pi_i(s) = \int_{-\infty}^s \pi_i(t) dt = \mathbb{E}_{\pi_i}(\mathbb{1}_{\mathcal{A}_s}(T)),$$

where $T \sim \pi_i$. Taking $\xi(x) = \mathbb{1}_{\mathcal{A}_s}(x)$ in (14) and using Theorem 1 produces a consistent estimator of the marginal distribution functions at any given point. Let X_t^i denote the i^{th} component of the Markov chain iteration X_t . For $s \in \mathbb{R}$, an estimator of $\Pi_i(s)$ is

$$\widehat{\Pi}_i(s) = \frac{\sum_{t=1}^n \mathbb{1}_{\mathcal{A}_s}(X_t^i) w^\lambda(X_t)}{\sum_{k=1}^n w^\lambda(X_k)}. \quad (19)$$

A quantile estimator is typically obtained by inverting the empirical distribution function using order statistics. This is not straightforward for unnormalized densities. To obtain a quantile estimator for the i^{th} component, consider the ordered sample $\{X_{i,(l)}\}$, where the notation $X_{i,(l)}$ defines the l^{th} order statistic obtained by sorting the entire d -tuple according to values in the i^{th} component. Denote

$$w_{(l)}^i = \frac{w^\lambda(X_{i,(l)})}{\sum_{t=1}^n w^\lambda(X_{i,(t)})}, \quad (20)$$

as the relative weights corresponding to the ordered sample observations for the i^{th} component. The estimator in (19) can then be rewritten in the following form that is more

amenable to inversion:

$$\hat{\Pi}_i(s) = \begin{cases} 0 & \text{if } s < X_{i,(1)} \\ \sum_{l=1}^m w_{(l)}^i & \text{if } X_{i,(m)} \leq s < X_{i,(m+1)} \\ 1 & \text{if } s \geq X_{i,(n)}. \end{cases}$$

Consequently, an importance sampling estimator of the α^{th} sample quantile for component i is,

$$\hat{x}_i^{(\alpha)} = \begin{cases} X_{i,(1)} & \text{if } \alpha = 0 \\ X_{i,(m)} & \text{if } \sum_{l=1}^{m-1} w_{(l)}^i < \alpha \leq \sum_{l=1}^m w_{(l)}^i. \end{cases} \quad (21)$$

The estimator in (21) can be cycled over all components for the desired quantiles to produce a complete set of credible intervals. Chen and Shao (1999) showed that if π is unimodal and $\{X_t\}_{t \geq 1}$ is a π^λ -ergodic Markov chain, then $\hat{x}_i^{(\alpha)}$ produces consistent credible intervals. Asymptotic normality of the estimators, however, has not been studied for when $\{X_t\}_{t \geq 1}$ is obtained via MCMC samples, and remains an open problem.

4.4 Tuning

The MY-IS estimator requires choosing a λ and Metropolis-Hastings tuning parameters. The parameter λ impacts performance of the estimator via the importance distribution while both impact the convergence of the π^λ -Markov chain. The latter is somewhat easier to address due to abundant guidelines available. We employ MALA and HMC algorithms for π^λ and follow the recommendations of Roberts and Rosenthal (1998) to tune MALA to attain approximately 57% acceptance and Beskos et al. (2013) to tune HMC to attain about 65% acceptance, respectively. The above is implemented after a value of λ is chosen,

fixing the MCMC target distribution. The choice for λ is a little more subtle as we describe below.

We choose λ with the aim to minimize the asymptotic variance in (16). Given a possibly non-smooth target density π , the importance density π^λ is smoother, encouraging faster mixing of the underlying MALA or HMC. Further, as we will motivate below, π^λ is expected to express reduced correlation across components compared to π , which in-turn facilitates sampling, leading to the variances in Σ being small. Therefore, larger values of λ will be more desirable from a sampling perspective. On the other hand, larger values of λ will increase the discrepancy between $\psi(x)$ and $\psi^\lambda(x)$ and consequently decrease $\mathbb{E}_{\pi^\lambda}(w^\lambda(X))$. This leads to increase in the variance, Ξ . There is thus a tension between choosing a large and small value of λ .

In the iid sampling scenario, there are guidelines for choosing the importance distribution based on the effective sample size² of Kong (1992) in importance sampling. Kong (1992) estimates the effective sample size of n samples from π^λ as

$$n_e = n \frac{\bar{w}_n^2}{w_n^2}, \quad (22)$$

where $\bar{w}_n^2 = n^{-1} \sum_{t=1}^n (w^\lambda(X_t))^2$. In iid sampling, an ideal choice of a proposal yields a reasonably high n_e/n . In our context, this suggests using a small λ but this would not necessarily yield any benefits in MCMC importance sampling. Similarly, a value of n_e/n close to 0 implies that the first moment of the weights is very small relative to the second moment, again unideal. Empirically, we find that choosing a value of λ such that

$$\frac{n_e}{n} \in [0.4, 0.8], \quad (23)$$

²Later, we will refer to another effective sample size in the context of MCMC samples. To avoid confusion, we denote the effective sample size in importance sampling as n_e .

typically balances the tradeoff between high and low values of λ .

A practitioner may start with an initial choice of λ_0 and adjust it until the weights yield n_e/n in the window above. A natural question is how to choose an initial λ_0 . This is challenging to answer in general, but fixing π to be the density of a Gaussian distribution, the following theorem indicates that the ideal λ scales linearly with dimension. Let Ω be a $d \times d$ positive-definite matrix and let $|\cdot|$ denote the determinant.

Theorem 4. Let π be the density of $N(0, \Omega)$. Then, the MY envelope density is the density of the $N(0, \Omega + \lambda \mathbb{I}_d)$ distribution. Further, let $s_1 \leq s_2 \leq \dots \leq s_d$ be the eigenvalues of Ω . Then for iid samples from π^λ , the value of λ corresponding to $\xi(x) = x$ that minimizes $\left| \lim_{n \rightarrow \infty} n \text{Var} \left(\hat{\theta}_n^{\text{MY}} \right) \right|$ is denoted by λ^* and satisfies

$$\sum_{i=1}^d \frac{\lambda^* d - s_i}{(s_i + \lambda^*)(s_i + 2\lambda^*)} = 0,$$

where,

$$\frac{s_1}{d} < \lambda^* < \frac{s_d}{d}.$$

Proof. See Appendix C. □

Thus, for higher dimensional problems, the initial value of λ can be chosen appropriately small. Theorem 4 also indicates that π^λ is better conditioned than π , which in-turn improves the performance of the underlying Markov chains (Roberts and Sahu, 1997). This becomes particularly beneficial for HMC algorithms as we will see in our numerical studies.

Remark 3. The optimal value of λ in Theorem 4 is for iid samples from π^λ . Under this framework, in Appendix C, we also obtain the value of n_e/n attained by this λ^* . Unsurprisingly, $n_e/n \rightarrow 1$ as $d \rightarrow \infty$. Such results are quite challenging to obtain for MCMC samples from π^λ , since a tractable expression of Σ in Ξ is unavailable.

5 Geometric ergodicity of Moreau-Yosida algorithms

We turn our attention to the conditions that guarantee MALA and HMC to yield a geometrically ergodic Markov chain for a Moreau-Yosida envelope density, π^λ . Properties of proximal operators help us arrive at simpler conditions for π^λ than what is generally available for π . As is standard in the literature, we also highlight the convergence behavior for a class of one-dimensional distributions $\mathcal{E}(\beta, \gamma)$. This class of distributions was first discussed in Roberts and Tweedie (1996) and provides a common ground to compare the performance with existing methods. For some $c \in \mathbb{R}$ and constants $\gamma > 0$ and $0 < \beta < \infty$, $\pi \in \mathcal{E}(\beta, \gamma)$ is of the form,

$$\pi(x) \propto \exp(-\gamma|x|^\beta), \quad |x| \geq c. \quad (24)$$

The value of β controls how quickly the tails of the distribution decay. It is further assumed that π is smooth enough for $|x| \leq c$ in order to satisfy basic differentiability assumptions. We state a general result for distributions in this class.

Result 1 (Pereyra (2016)). Assume that $\pi \in \mathcal{E}(\beta, \gamma)$ with $\beta \geq 1$. Then $\pi^\lambda \in \mathcal{E}(\beta', \gamma')$ with $\beta' = \min(\beta, 2)$ and some $\gamma' > 0$.

Pereyra (2016) does not provide the value of γ' , however we note that for distributions of the form (24) having $\psi(x) = \gamma|x|^\beta$,

$$\psi^\lambda(x) = \min_{y \in \mathbb{R}} \left\{ \gamma|y|^\beta + \frac{1}{2\lambda}(x - y)^2 \right\}. \quad (25)$$

When $\beta > 2$, the first term in the minimization (25) dominates the second quadratic term pushing the minimization to occur at $y \approx 0$. When $\beta < 2$, the minimization tends to occur at $y \approx x$ due to the dominance of the quadratic term. The minimizer for $\beta = 2$

case is obtained exactly where the derivative of the objective function in (25) vanishes. Consequently, for large x ,

$$\gamma' = \begin{cases} \gamma & \text{if } \beta < 2 \\ \frac{\gamma}{1+2\gamma\lambda} & \text{if } \beta = 2 \\ \frac{1}{2\lambda} & \text{if } \beta > 2. \end{cases} \quad (26)$$

Result 1 ensures that when $\pi \in \mathcal{E}(\beta, \gamma)$, then $\pi^\lambda \in \mathcal{E}(\beta', \gamma')$. Critically, when π has lighter than Gaussian tails, π^λ has Gaussian tails. This will be critical to understanding the convergence behavior of π^λ -MALA and π^λ -HMC algorithms.

5.1 Metropolis-adjusted Langevin algorithms

Roberts and Tweedie (1996) provide sufficient conditions for geometric ergodicity of a MALA algorithm given a general target π . We apply their results to π^λ . Let $q_M(x, y)$ denote the density of a MALA proposal for a target π , i.e., $q_M(x, y)$ is the density of $N(x + h\nabla \log \pi(x)/2, h\mathbb{I}_d)$. Let $A(x)$ denote the acceptance region where a proposed value is guaranteed to be accepted. That is,

$$A(x) = \left\{ y : \frac{\pi(y)q_M(y, x)}{\pi(x)q_M(x, y)} \geq 1 \right\}. \quad (27)$$

Let $R(x) = A(x)^c$ denote the potential rejection region, where there is a positive probability of rejection. Let $I(x)$ denote the set of points interior to x , i.e.,

$$I(x) = \{y : \|y\| \leq \|x\|\}. \quad (28)$$

Finally, let $A(x)\Delta I(x)$ denote the symmetric difference between $A(x)$ and $I(x)$.

Theorem 5 (Roberts and Tweedie (1996)). Assume $A(\cdot)$ converges inwards in q , i.e.,

$$\lim_{\|x\| \rightarrow \infty} \int_{A(x)\Delta I(x)} q_M(x, y) dy = 0. \quad (29)$$

Let $c(x) = x + h\nabla \log \pi(x)/2$ denote the mean of the proposal. If

$$\eta := \liminf_{\|x\| \rightarrow \infty} \{\|x\| - \|c(x)\|\} > 0, \quad (30)$$

then the MALA chain is geometrically ergodic for π .

Due to the specific structure of $\nabla \log \pi^\lambda$, condition (30) can be met as long as the following assumption is satisfied.

Assumption 1. For a target density π of the form (1) with $\psi \in \Gamma(\mathbb{R}^d)$, we assume

$$\limsup_{\|x\| \rightarrow \infty} \frac{\|\text{prox}_\psi^\lambda(x)\|}{\|x\|} = l < 1. \quad (31)$$

Theorem 6. Let the target density be π^λ so that $c(x) = x - h\nabla \psi^\lambda(x)/2$. Assume that $A(\cdot)$ converges inwards. Then if $h \leq 2\lambda$, the π^λ -MALA chain is geometrically ergodic.

Proof. See Appendix D.1. □

Remark 4. Pereyra (2016) does not employ the condition in Assumption 1 and instead state that for $\psi \in \Gamma(\mathbb{R}^d)$, $\|\text{prox}_\psi^\lambda(x)\| < \|x\|$ for all x . Unfortunately, this is not true in general. Consider $\psi(x) = (x - 5)^2$, corresponding to a Gaussian density centered at 5. Here

$$\text{prox}_\psi^\lambda(x) = x \frac{1}{1 + 2\lambda} + 5 \frac{2\lambda}{1 + 2\lambda}.$$

For $0 < x < 5$, $|\text{prox}_\psi^\lambda(x)| > |x|$, and this observation is true for many target densities that

are not maximized at 0. Further, in the event that for a target density, $\|\text{prox}_\psi^\lambda(x)\| < \|x\|$ is true for all x (except $x \neq 0$), this is not sufficient to ensure η in (30) is positive, since the \liminf can still be zero.

We instead employ the sufficient condition in Assumption 1. Many log-concave target densities satisfy this condition. A known exception is the Laplace density, for which even the original conditions of Theorem 5 are not satisfied. However, as will discuss subsequently, geometric ergodicity in this case still holds using alternative results in Roberts and Tweedie (1996). Assumption 1 is also sufficient to yield the geometric ergodicity results of Pereyra (2016).

Remark 5. If $l = 0$ in Assumption 1, as it is often for light-tailed distributions, then it is possible to modify the proof so that under the assumption of $A(\cdot)$ converging inwards and with a choice of $h \leq 4\lambda$, π^λ -MALA is geometrically ergodic.

Theorem 6 alleviates the burden of verifying (30) since a judicious choice of h ensures condition (30) is satisfied. Condition (29) is common and indicates that in the tails, the algorithm should either propose a value in the rejection region or propose a point moving away from the tails that is sure to be accepted. Livingstone et al. (2019) highlight that this condition is important to “limit the degree of oscillation in the tails” of the target density. Roberts and Tweedie (1996) explain that the condition is connected to convexity of ψ^λ . Verification of the condition is typically done for different models on a case-by-case basis. In addition to a general target, Theorem 6 and Result 1 provide significant improvement for $\pi \in \mathcal{E}(\beta, \gamma)$ as well.

1. If $\beta \in [1, 2)$ then $\beta' = \beta$. MALA is geometrically ergodic for both π and π^λ by Meyn and Tweedie (2012, Section 16.1.3) and Roberts and Tweedie (1996, Theorem 4.1).
2. If $\beta = 2$ then $\beta' = 2$. According to Roberts and Tweedie (1996) π^λ -MALA is

geometrically ergodic when $h\gamma' < 2$. Therefore, π^λ -MALA is geometrically ergodic if $h < 4\lambda + 2/\gamma$.

3. If $\beta > 2$ then by (11) π -MALA is not geometrically ergodic. However in this case, for π^λ , $\beta' = 2$ with $\gamma' = 1/(2\lambda)$. Consequently, the π^λ -MALA chain is geometrically ergodic as long as $h \leq 4\lambda$. This is consistent with Remark 5.

For $\beta > 2$, the target π corresponds to distributions with tails lighter than Gaussian. In such cases, efficient implementation of gradient-based schemes becomes difficult. Consequently, it becomes challenging to obtain a geometrically ergodic Markov chain. Livingstone and Zanella (2022) proposed a Barker’s algorithm to mitigate this problem. In Section 6.4 for a light-tailed differentiable target, we compare our proposed MY-IS strategy with the Barker’s algorithm as well.

5.2 Hamiltonian Monte Carlo

Hamiltonian Monte Carlo is a gradient-based MCMC algorithm that has enjoyed success in a variety of problems. For a given target, $\pi(x) \propto e^{-\psi(x)}$, the HMC proposal is constructed by (approximately) conserving the total energy or Hamiltonian,

$$H(x, z) = \psi(x) + \frac{1}{2}z^T M^{-1}z.$$

Here, z is a d -dimensional augmented momentum variable (see Neal, 2011; Betancourt et al., 2017, for details) and M is a $d \times d$ positive-definite mass matrix. We will fix $M = \mathbb{I}_d$. Let $L \geq 1$ be an integer representing the number of leapfrog steps in the approximation of the Hamiltonian dynamics and let $\varepsilon > 0$ be a step-size. For a current state x_0 and $z_0 \sim N(0, \mathbb{I}_d)$, Livingstone et al. (2019) elucidate that the HMC proposal for a target π

can be expressed as

$$x_{L\varepsilon} = x_0 - \frac{L\varepsilon^2}{2}\nabla\psi(x_0) - \varepsilon^2 \sum_{i=1}^{L-1} (L-i)\nabla\psi(x_{i\varepsilon}) + L\varepsilon z_0, \quad (32)$$

where $x_{i\varepsilon}$ is the state at the i^{th} leapfrog step. We will denote the mean of the proposed value as $m_{L,\varepsilon}(x_0, z_0) = x_0 - (L\varepsilon^2/2)\nabla\psi(x_0) - \varepsilon^2 \sum_{i=1}^{L-1} (L-i)\nabla\psi(x_{i\varepsilon})$, so that $x_{L\varepsilon} = m_{L,\varepsilon}(x_0, z_0) + L\varepsilon z_0$. Let $q_{\text{H}}(x_0, \cdot)$ denote the density of the HMC proposal. Define the potential rejection region as

$$R(x) = \left\{ y : \frac{\pi(y)q_{\text{H}}(y, x)}{\pi(x)q_{\text{H}}(x, y)} \leq 1 \right\}. \quad (33)$$

Sufficient conditions for geometric ergodicity for HMC were provided in Livingstone et al. (2019). The following assumption is made on L to ensure irreducibility of the Markov chain.

Assumption 2. The number of leapfrog steps L is chosen using a distribution $\mathcal{L}(\cdot)$ such that $\Pr_{\mathcal{L}}[L = 1] > 0$ and for any $(x_0, z_0) \in \mathbb{R}^{2d}$ and $\varepsilon > 0$, there is an $s < \infty$ such that $\mathbb{E}_{\mathcal{L}}[e^{s\|x_{L\varepsilon}\|}] < \infty$.

Theorem 7 (Livingstone et al. (2019)). The HMC algorithm produces a π -geometrically ergodic Markov chain if Assumption 2 holds and in addition for $\eta(d) = \Gamma((d+1)/2)/\Gamma(d/2)$, $1/2 < \delta < 1$,

$$\limsup_{\|x\| \rightarrow \infty, \|z\| \leq \|x\|^\delta} \{ \|m_{L,\varepsilon}(x, z)\| - \|x\| \} < -\sqrt{2}L\varepsilon\eta(d), \quad (34)$$

and

$$\lim_{\|x\| \rightarrow \infty} \int_{R(x) \cap I(x)} q_{\text{H}}(x, y) dy = 0. \quad (35)$$

Remark 6. Condition (35) is similar to (29) but a little weaker, requiring that when at the tails of the distribution, the proposal should not propose a move away from the tails that could possibly be rejected.

Condition (34) can be challenging to verify, and hence Livingstone et al. (2019) provide the following sufficient conditions for it to hold.

Theorem 8 (Livingstone et al. (2019)). For any $L \geq 1$, (34) holds if the following are met

$$(a) \quad \lim_{\|x\| \rightarrow \infty} \|\nabla\psi(x)\| = \infty, \quad (36)$$

$$(b) \quad \liminf_{\|x\| \rightarrow \infty} \frac{\langle \nabla\psi(x), x \rangle}{\|\nabla\psi(x)\| \|x\|} > 0, \quad (37)$$

$$(c) \quad \lim_{\|x\| \rightarrow \infty} \frac{\|\nabla\psi(x)\|}{\|x\|} = 0. \quad (38)$$

In addition, if (c) is replaced by,

$$(c^*) \quad \limsup_{\|x\| \rightarrow \infty} \frac{\|\nabla\psi(x)\|}{\|x\|} = S_l, \quad (39)$$

for some $S_l < \infty$, then there exists an $\varepsilon_0 < \infty$ such that (34) holds provided $\varepsilon < \varepsilon_0$.

As it turns out, under Assumption 1, (36), (37), and (39) hold for π^λ , and verifying geometric ergodicity is significantly simpler.

Theorem 9. Suppose Assumption 1 and Assumption 2 hold. Then π^λ -HMC algorithm is geometrically ergodic for a sufficiently small ε , if

$$\lim_{\|x\| \rightarrow \infty} \int_{R(x) \cap I(x)} q_H(x, y) dy = 0. \quad (40)$$

Proof. See Appendix D.2. □

We recognize that as it is true for general targets, demonstrating (40) can be challenging

to establish for general problems. We have, however, some guiding principles based on π 's tail behavior when π belongs to the exponential family class $\mathcal{E}(\beta, \gamma)$.

1. If $\beta \in [1, 2)$ then $\beta' = \beta$. By the result of Livingstone et al. (2019), π^λ -HMC is geometrically ergodic.
2. If $\beta = 2$ then $\beta' = 2$ and π -HMC is geometrically ergodic for sufficiently small ε . Consequently, π^λ -HMC is also geometrically ergodic for sufficiently small ε .
3. If $\beta > 2$ then π -HMC is not geometrically ergodic (Livingstone et al., 2019). However for π^λ , $\beta' = 2$, and thus π^λ -HMC is geometrically ergodic for sufficiently small ε .

6 Numerical studies

We evaluate our proposed methodology in a variety of simulation studies. Continuing from the toy example in Figure 1, we study the effectiveness of the importance sampling scheme for univariate and multivariate targets in $\mathcal{E}(\beta, 1)$. This first study clarifies the impact of different λ on the quality of estimation. Next, we consider a Bayesian trendfiltering problem. The goal in this problem is efficient uncertainty quantification of posterior estimates when the posterior distribution is non-differentiable. We then consider a 4096-dimensional image denoising problem, demonstrating the effectiveness of the MY-IS estimator in high dimensions. Finally, we consider a Bayesian Poisson random effects model. Here, the posterior is differentiable but has thin tails. This is a well known scenario where standard gradient-based MCMC methods struggle.

In all studies we tune λ following the guidelines in Section 4.4. We implement MY-IS with both π^λ -MALA and π^λ -HMC samples. We compare Markov chains π^λ -MALA with P-MALA of Pereyra (2016) and π^λ -HMC with P-HMC of Chaari et al. (2016). For the Bayesian Poisson random effects model, Livingstone and Zanella (2022) show that the

traditional MALA algorithm is unreliable and demonstrate the superiority of their Barker’s algorithm. We compare π^λ -MALA and π^λ -HMC chains with the Barker’s algorithm as well. Implementation details of these algorithms are provided in Appendix E.1.

We evaluate the methods on their statistical efficiency by comparing variances of estimators of the posterior means. Specifically, we calculate relative efficiency of Method 1 over Method 2 as follows

$$\text{eff}^{\text{rel}} = \frac{1}{p} \sum_{i=1}^p \frac{\hat{\tau}_{i(\text{Method 2})}^2}{\hat{\tau}_{i(\text{Method 1})}^2},$$

where $\hat{\tau}_{i(\cdot)}^2$ denotes the estimated asymptotic variance of component i from the respective method. R code for reproducing all studies is available at <https://github.com/sapratim/MoreauYosidaMCMC-IS>.

6.1 Toy example

Consider the target distribution with density

$$\pi_\beta(x_1, \dots, x_d) \propto \prod_{i=1}^d e^{-\psi_\beta(x_i)} = \prod_{i=1}^d e^{-|x_i|^\beta}, \quad x_i \in \mathbb{R}, \quad (41)$$

$i = 1, 2, \dots, d$, for $\beta = 1$ (Laplace) and $\beta = 4$ (super-Gaussian). Then $\psi(x) = \sum_{i=1}^d |x_i|^\beta$, and its Moreau-Yosida envelope is

$$\psi_\beta^\lambda(x) = \min_{y \in \mathbb{R}^d} \left(\sum_{i=1}^d |y_i|^\beta + \frac{1}{2\lambda} \|x - y\|^2 \right). \quad (42)$$

Recall that the i^{th} component of the proximal mapping of a separable sum of functions is the proximal mapping of the i^{th} function in the sum (Parikh et al., 2014), i.e.,

$$\text{prox}_{\psi_\beta}^\lambda(x_i) = \arg \min_{y_i \in \mathbb{R}} \left(|y_i|^\beta + \frac{1}{2\lambda}(x_i - y_i)^2 \right).$$

For $\beta = 1$, we obtain the familiar soft-thresholding function

$$\text{prox}_{\psi_1}^\lambda(x_i) = \begin{cases} (|x_i| - \lambda)\text{sgn}(x_i) & \text{if } |x_i| \geq \lambda \\ 0 & \text{otherwise.} \end{cases}$$

Durmus et al. (2022) provide the exact expression of π_1^λ for $d = 1$:

$$\pi_1^\lambda(x) = \frac{\exp \left\{ \left(\frac{\lambda}{2} - |x| \right) \mathbb{1}(|x| \geq \lambda) - \frac{x^2}{2\lambda} \mathbb{1}(|x| < \lambda) \right\}}{2(e^{-\lambda/2} + \sqrt{2\pi\lambda}(\Phi(\sqrt{\lambda}) - 1/2))}.$$

For $\beta = 4$, we obtain

$$\text{prox}_{\psi_4}^\lambda(x_i) = \frac{\sqrt[3]{3} \left(\sqrt{3} \sqrt{\lambda^3(27\lambda x_i^2 + 1)} + 9\lambda^2 x_i \right)^{\frac{2}{3}} - 3^{\frac{2}{3}} \lambda}{6\lambda \sqrt[3]{\sqrt{3} \sqrt{\lambda^3(27\lambda x_i^2 + 1)} + 9\lambda^2 x_i}}, \quad (43)$$

which yields an expression of π_4^λ up to a normalization constant.

We investigate the effect of λ on the π^λ -MALA Markov chain and the quality of the importance sampling estimator $\hat{\theta}_n^{\text{MY}}$ for dimensions $d = 1, 10$, and 20 . For every combination of β and d , we track the following as λ is varied: (i) the estimated n_e/n , which reflects the quality of the importance sampling proposal, π^λ , (ii) the MCMC effective sample size by n for estimating the mean of π^λ , which reflects the mixing quality of the π^λ -Markov chain, and (iii) the estimated asymptotic variance of the MY-IS estimator. Each Markov

chain is run for $n = 10^6$ iterations. Figure 2 shows these quantities as a function of λ when $\beta = 1$, and Figure 3 shows them when $\beta = 4$.

We see similar trends for both values of β . As λ increases, n_e/n decreases, the MCMC effective sample size for π^λ improves and the trade-off between these two is balanced by the variance of the MY-IS estimator. Our recommendation of choosing λ such that n_e/n is in $[0.40, 0.80]$ holds up in these examples.

6.2 Bayesian trendfiltering

Consider the standard task in nonparametric regression. Let $y(t)$ be a scalar function of time that is a superposition of a smooth function $\mu(t)$ and additive noise. The function $y(t)$ is observed at time points t_1, \dots, t_m , and one models $y = (y(t_1), \dots, y(t_m))^\top$ as

$$y = \mu + \epsilon, \tag{44}$$

where $\mu = (\mu(t_1), \dots, \mu(t_m))^\top$ and $\epsilon \sim N(0, \sigma^2 \mathbb{I}_m)$. The goal is to recover $\mu \in \mathbb{R}^m$ from the observations $y \in \mathbb{R}^m$.

Kim et al. (2009) proposed ℓ_1 -trendfiltering, which estimates μ with the solution to the following convex optimization problem

$$\underset{\mu \in \mathbb{R}^m}{\text{minimize}} \quad \frac{1}{2} \|y - \mu\|^2 + \alpha \left\| \mathbb{D}_m^{(k+1)} \mu \right\|_1. \tag{45}$$

The nonnegative regularization parameter α trades off model fit quantified by the quadratic term and model complexity quantified by the ℓ_1 -penalty on the roughness of $\mu(t)$. Specifically, $\mathbb{D}_m^{(k+1)} \in \mathbb{R}^{(m-(k+1)) \times m}$ is a discrete difference matrix of order $(k+1)$ and dimension

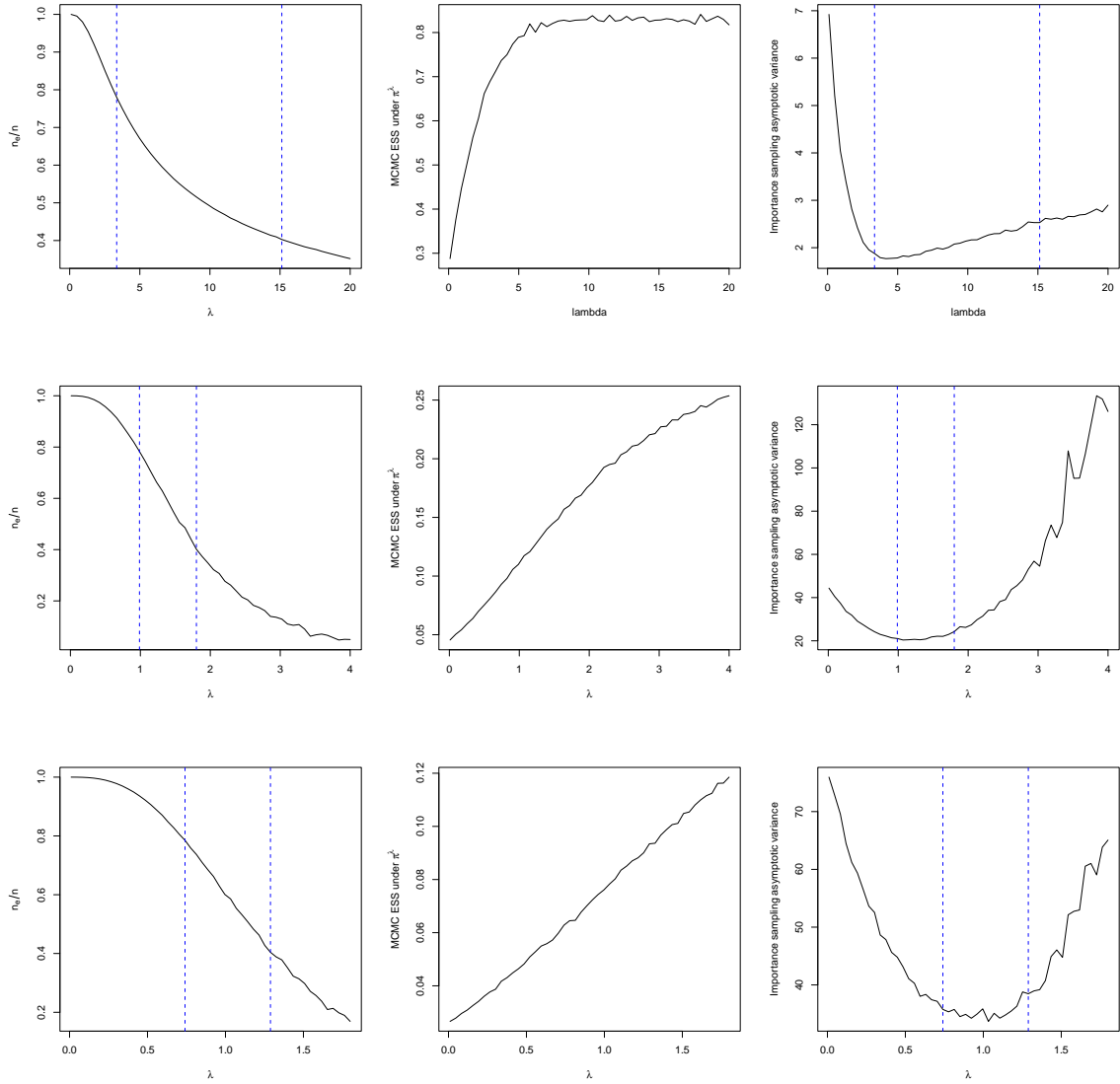


Figure 2: (Laplace) From top to bottom $d = 1, 10, 20$. Left column has the importance sampling effective sample size n_e/n for different λ , middle column has the MCMC effective sample size for the π^λ -MALA chain for different λ , and the right column has the estimated importance sampling asymptotic variance for different values of λ . The two vertical lines are the values of λ that yield $n_e/n \in \{0.40, 0.80\}$.

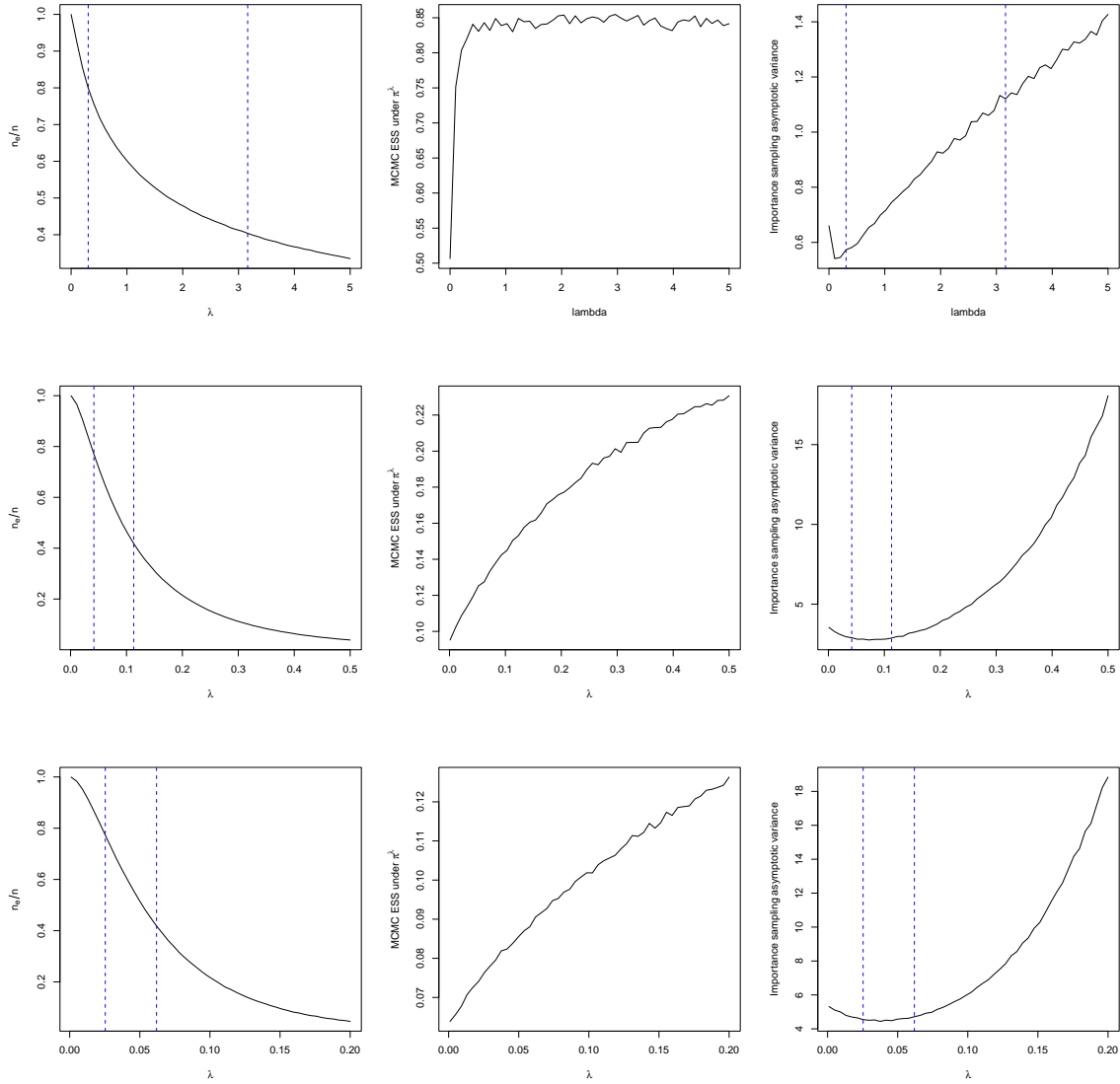


Figure 3: (Super-Gaussian) From top to bottom $d = 1, 10, 20$. Left column has the importance sampling effective sample size n_e/n for different λ , middle column has the MCMC effective sample size for the π^λ -MALA chain for different λ , and the right column has the estimated importance sampling asymptotic variance for different values of λ . The two vertical lines are the values of λ that yield $n_e/n \in \{0.40, 0.80\}$.

m . For $k = 0$,

$$D_m^{(1)} = \begin{pmatrix} -1 & 1 & 0 & \dots & 0 & 0 \\ 0 & -1 & 1 & \dots & 0 & 0 \\ \vdots & \vdots & \ddots & \ddots & \vdots & \vdots \\ 0 & 0 & \dots & -1 & 1 & 0 \\ 0 & 0 & \dots & 0 & -1 & 1 \end{pmatrix} \in \mathbb{R}^{(m-1) \times m}.$$

The function $\|D_m^{(1)}\mu\|_1 = \sum_{i=1}^{m-1} |\mu_{i+1} - \mu_i|$ is the fused lasso penalty (Tibshirani et al., 2005), which is designed to recover piecewise constant μ . When $k = 1, 2$, and 3 , the penalty incentivizes the recovery of piecewise linear, quadratic, and cubic trends, respectively. Difference matrices can be calculated recursively by the relation $D_m^{(k+1)} = D_{m-k}^{(1)} D_m^{(k)}$. The solution to (45) produces the maximum a posteriori (MAP) estimator corresponding to an appropriate Bayesian model. Later works proposed approaches that not only produce point estimates but also can quantify the uncertainty in those estimates (Roualdes, 2015; Faulkner and Minin, 2018; Kowal et al., 2019; Heng et al., 2023). We work in the latter context and consider a Bayesian model with the following posterior distribution that corresponds to the MAP estimate computed in (45),

$$\pi(\mu|y) \propto \exp \left\{ -\frac{\|y - \mu\|^2}{2\sigma^2} - \alpha \|D_m^{(k+1)}\mu\|_1 \right\}. \quad (46)$$

The ℓ_1 -penalty renders the posterior non-differentiable, precluding the use of traditional gradient-based MCMC schemes. Thus, the posterior in (46) is a natural candidate for a proximal MCMC-type sampler.

Following model (44), we set $\sigma^2 = 9$ and for $m = 100$ obtain equally spaced time points

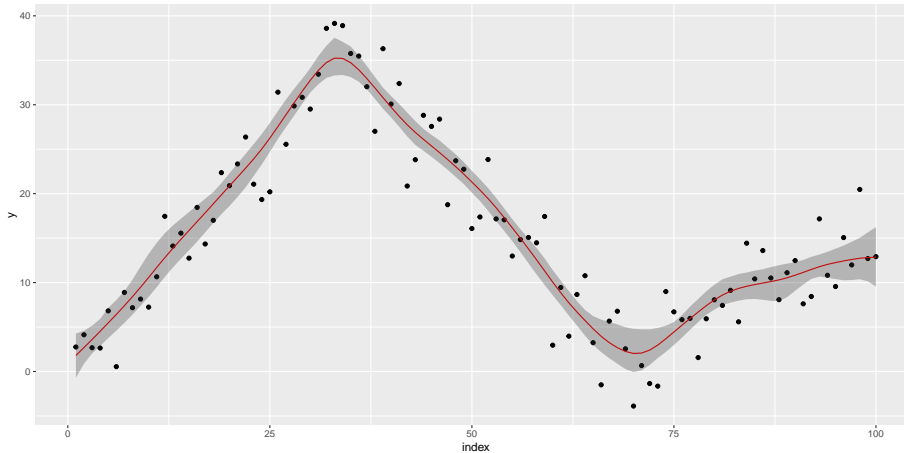


Figure 4: Trend filtering fit using the marginal quantiles and posterior mean (*in red*) for importance sampling estimator.

from

$$\mu(t) = \begin{cases} t, & \text{if } t \leq 35 \\ 70 - t, & \text{if } t \leq 70 \\ 0.5t - 35, & \text{otherwise.} \end{cases}$$

Figure 4 shows the posterior mean and a band of 95% credible intervals computed by MY-IS, with the latter derived using (21).

We compare four proximal MCMC algorithms: (i) P-MALA, (ii) P-HMC, (iii) π^λ -MALA, and (iv) π^λ -HMC. For the latter two chains, we set $\lambda = 0.001$ to obtain an importance sampling effective sample size of $n_e/n \approx 0.47$. For all chains we simulate a Monte Carlo sample size of $n = 10^5$. We ran 100 replications of all four Markov chains to ascertain the gains in relative efficiencies.

Figure 5 shows the average relative efficiency of P-MALA versus IS-MALA (left) and P-HMC versus IS-HMC (right) in box plots of the 100 components. For HMC, estimation

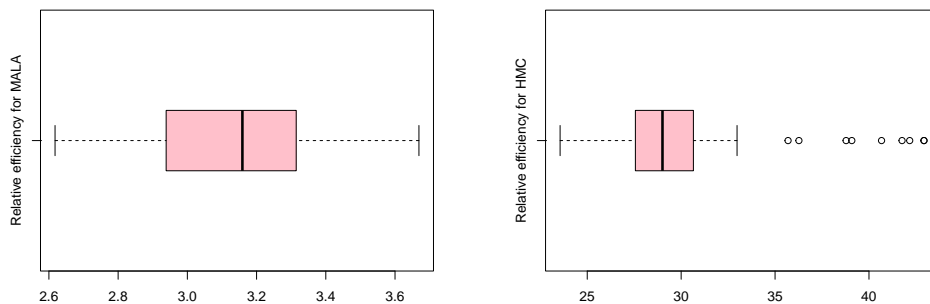


Figure 5: Trendfiltering: Average relative efficiencies of IS-MALA over P-MALA (left) and IS-HMC over P-HMC (right).

of components are at least 25 times more efficient. For MALA it is at least 2.6 times more efficient. The gains in efficiency with importance sampling are significant, especially in the case of π^λ -HMC. To better understand these differences in efficiency gains, we examine the ability of MALA and HMC algorithms to explore π^λ compared to π . Specifically, we compute the difference in the estimated autocorrelation lags between pairs of algorithms, i.e., the difference between their autocorrelation functions (ACFs). Figure 6 presents the ACF difference plot computed using samples from P-MALA and π^λ -MALA (left) and P-HMC and π^λ -HMC (right) in a box plot over the 100 components of the chains. For MALA, some components show improved mixing, whereas other components show marginally slower mixing. Despite this, the use of importance sampling yields significant gains as was seen in Figure 5. In contrast, for HMC, all components exhibit substantially improved mixing of π^λ -HMC.

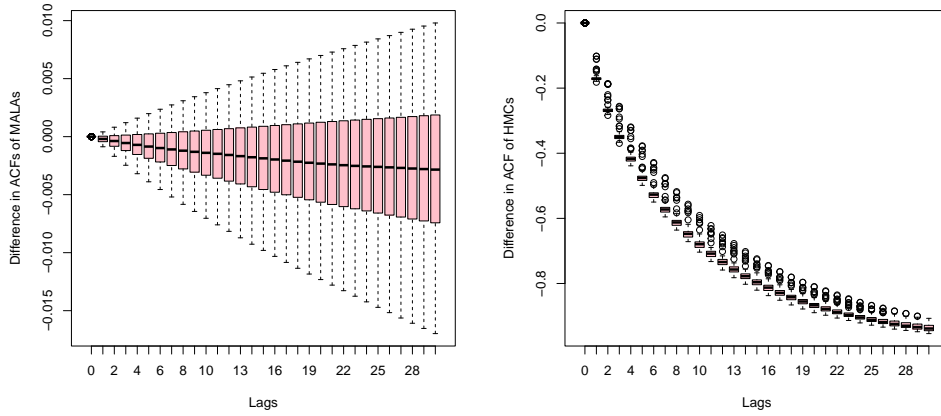


Figure 6: Trendfiltering: ACF difference plots computed using samples from π^λ -MALA and P-MALA (left), π^λ -HMC and P-HMC (right).

6.3 Nuclear-norm based low rank matrix estimation

Estimating low rank matrices is a fundamental problem in statistics. A classic penalized likelihood approach to recovering low rank matrices is to employ a nuclear norm regularization term (Fazel, 2002). For example, the nuclear norm has been used in this role for regularized matrix regression (Zhou and Li, 2013), matrix linear discriminant analysis (Hu et al., 2020), and matrix completion (Mazumder et al., 2010; Cai et al., 2010). For illustrative purposes, we consider the problem of estimating a low-rank matrix in the context of matrix denoising.

We observe a matrix $Y \in \mathbb{R}^{m \times k}$ where $Y = X + E$. The matrix X is a latent low-rank matrix that we wish to recover and E is a noise matrix with iid Gaussian entries, i.e., $e_{ij} \sim N(0, \sigma^2)$. We assume the following prior on X

$$\pi(X) \propto \exp(-\alpha \|X\|_*), \quad (47)$$

where $\|X\|_*$ is the nuclear norm of X . Having observed Y , the posterior density of X is

$$\pi(X|Y) \propto \exp \left\{ - \left(\frac{\|Y - X\|_F^2}{2\sigma^2} + \alpha \|X\|_* \right) \right\}, \quad (48)$$

where $\|X\|_F$ denotes the Frobenius norm of X . Assuming low-rank structure is quite natural for matrix denoising tasks. For example, in the context of video denoising, assuming X has low-rank structure is reasonable since its columns, which are vectorized frames in a video sequence, are typically highly correlated. As in the trendfiltering example, a non-smooth penalty renders the target posterior non-differentiable, precluding the use of traditional gradient-based MCMC schemes. Thus, the posterior in (48) is also a natural candidate for a proximal MCMC-type sampler. Recht et al. (2010) derived the proximal mapping of the negative log-posterior in (48):

$$\text{prox}_\psi^\lambda(X) = \text{SVT} \left(\frac{\lambda}{\lambda + \sigma^2} Y + \frac{\sigma^2}{\lambda + \sigma^2} X, \frac{\alpha \lambda \sigma^2}{\lambda + \sigma^2} \right). \quad (49)$$

The mapping $\text{SVT}(Z, t)$ is the singular value soft thresholding operator. Let $Z = UDV^\top$ denote a singular value decomposition of Z where D is a diagonal matrix of singular values. Let d_i denote the i^{th} singular value of D . Let \tilde{D} be the matrix obtained by replacing the i^{th} singular value of D by $\max\{d_i - t, 0\}$. Then $\text{SVT}(Z, t) = U\tilde{D}V^\top$. In the following numerical studies, we take X to be the checkerboard image of 64×64 pixels studied in Pereyra (2016). Note that this is a relatively high-dimensional Bayesian inference problem as the dimension of the posterior distribution is 4096 (64^2). Additional details on the data are in Appendix E.3. We set $\sigma^2 = 0.01$ and following Pereyra (2016), set $\alpha = 1.15/\sigma^2$. Setting $\lambda = 10^{-4}$ we obtain an importance sampling effective sample size of $n_e/n \approx 0.41$. For all chains we simulate a Monte Carlo sample size of $n = 10^5$ and ran 100 replications of all chains to ascertain the gains in relative efficiencies. We present

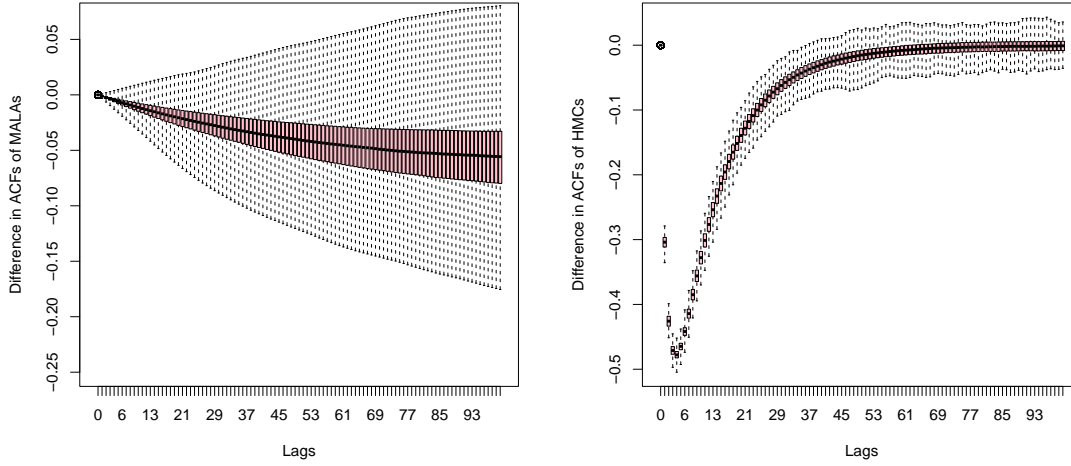


Figure 7: Nuclear-norm based matrix denoising: ACF difference plots computed using samples from π^λ -MALA and P-MALA (*left*), π^λ -HMC and P-HMC (*right*).

ACF difference plots from a randomly selected single replicate. For the ACF plots we obtain component-wise autocorrelations and present boxplots of component-wise difference in ACFs of P-MALA $-\pi^\lambda$ -MALA (same for HMC). For the relative efficiencies, we average the relative efficiencies over the 100 replications and present a boxplot of the average relative efficiencies over all components.

As previously observed in Pereyra (2016), P-MALA works well in this example. This can be seen in Figure 7, where the difference in the ACFs for the P-MALA and π^λ -MALA chains is marginally significant. However, Figure 8 indicates that the MY-IS procedure nonetheless yields a more efficient estimator. In the case of HMC, the improved efficiency is even better. Figure 7 indicates a significant improvement in the ACF behavior for the π^λ -HMC chain over the P-HMC chain, which leads to a significant gain in relative efficiency as demonstrated in Figure 8.

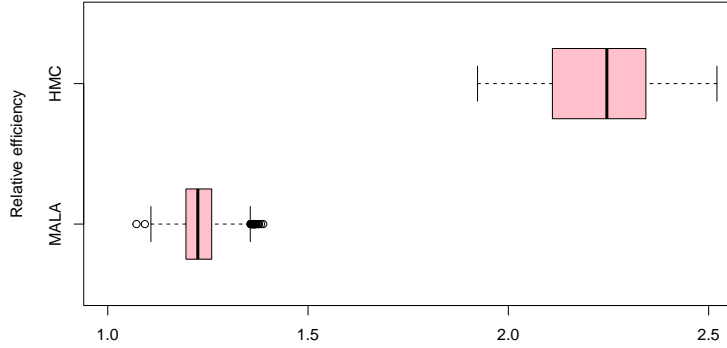


Figure 8: Nuclear-norm based matrix denoising: Average relative efficiencies of π^λ -MALA over P-MALA and π^λ -HMC over P-HMC.

6.4 Bayesian Poisson random effects model

We revisit the Bayesian Poisson random effects model presented in Livingstone and Zanella (2022). MALA and HMC struggle to reliably generate samples from this model’s posterior due to its light tails. Their proposed Barker’s algorithm, however, can successfully generate samples in spite of the light tails. Given the effect of Moreau-Yosida smoothing on the exponential family class $\mathcal{E}(\beta, \gamma)$, one might conjecture that our MY-IS scheme could also be robust to light tails. Consequently, we test this conjecture by estimating the posterior mean with our MY-IS scheme.

The model has the following hierarchical specification:

$$\begin{aligned}
 y_{ij} \mid \eta_i &\sim \text{Poisson}(e^{\eta_i}) & j = 1, 2, \dots, n_i, \\
 \eta_i \mid \mu &\sim \text{N}(\mu, \sigma_\eta^2) & i = 1, 2, \dots, I, \\
 \mu &\sim \text{N}(0, c^2),
 \end{aligned}$$

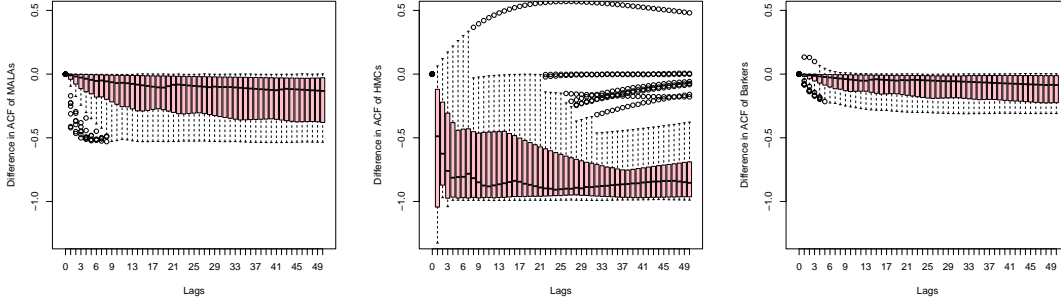


Figure 9: Poisson random effects model: ACF difference plots computed using samples from π^λ -MALA and P-MALA (left), π^λ -HMC and P-HMC (center) and π^λ -Barker and P-Barker (right).

where y_{ij} represent count data measured for the j^{th} subject in the i^{th} class, with n_i being the number of subjects in the i^{th} class. Following Livingstone and Zanella (2022), we set the number of classes I to be 50, $\sigma_\eta = 3$, and $c = 10$. In Appendix E.4, we present an efficient algorithm to evaluate the Moreau-Yosida envelope. In contrast to the previous examples, this posterior density is differentiable. Thus, we also compare our results with those obtained using Barker’s algorithm. We set $\lambda = 0.001$ to obtain an importance sampling effective sample size of $n_e/n \approx 0.41$. For all chains we simulate a Monte Carlo sample size of $n = 10^5$ and ran 100 replications of all chains to ascertain the gains in relative efficiencies. As before, we show the ACF difference plots from a randomly selected single replicate. This time we also compare Barker’s algorithm with π^λ -Barker’s algorithm. Figure 9 shows that all three π^λ chains mix better than their counterparts in general. There is one component whose mixing is better in P-HMC and Barker’s, but for all other components there is a significant improvement in the quality of the Markov chains. Particularly, π^λ -HMC demonstrates significant improvement.

To demonstrate the impact of using MY-IS, we also present the relative efficiencies, focusing also on the relative efficiency of MY-IS using Barker’s algorithm versus π^λ -MALA.

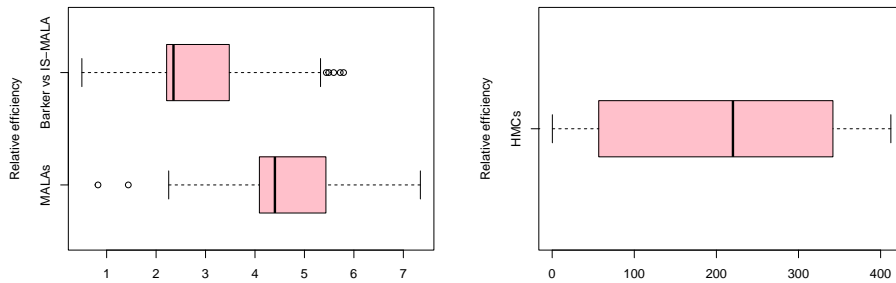


Figure 10: Poisson random effects model: Average relative efficiencies of π^λ -MALA over P-MALA and π^λ -MALA over P-Barker (*left*) and π^λ -HMC over P-HMC (*right*).

Similar to other examples, we run 100 replications for $n = 10^5$ length Markov chains. The box plot in Figure 10 presents the average relative efficiencies across components. First, we note the significant gains in efficiency using π^λ -HMC. This corroborates our conjecture that π^λ 's heavier tails make it more conducive for HMC to traverse the space. We also note that MY-IS using MALA chains also significantly improves efficiency, compared to both P-MALA and Barker's algorithm, with almost all components exhibiting relative efficiency above 1.

7 Discussion

The problem of non-differentiability of the target density is a key obstacle in building effective MCMC strategies. In this work, we propose an importance sampling paradigm for a class of log-concave targets using Moreau-Yosida envelopes as a proposal. Our proposed estimator is guaranteed to have finite variance, with a Markov chain that can often mix better on the proposal than the original target. We demonstrate the gains in efficiency using our proposed methodology over a variety of examples and highlight the utility of

employing π^λ -MCMC with importance sampling.

Although most applications of importance sampling use iid samples from the importance distribution, MCMC samples from the importance distribution have also been employed with some success (see for example Liesenfeld and Richard, 2008; Richard and Zhang, 2007; Osmundsen et al., 2021; Schuster and Klebanov, 2020). However, their use is either in specific problems, low-dimensional settings, or without the guarantee of finite variance of estimators. Adaptive importance sampling methods with MCMC samples are also common in signal processing (Martino et al., 2018; Llorente et al., 2022) but their application is also typically limited to low-dimensional multi-modal target distributions. Concurrently with our work, Elvira et al. (2024) identify the use of proximal mappings in developing effective adaptive importance sampling paradigms for non-differentiable targets through a proximal Newton adaptation strategy.

The application of our proposed methodology, and indeed any proximal MCMC methodology, is initially focused on log-concave distributions due to the availability of efficient global solvers for the proximal mapping. Nonetheless, for π that is not log-concave, it may be possible to choose λ so that π^λ is log-concave. This would enable our MY-IS estimator to apply to much a wider class of target densities. The choice of λ here is crucial and critically dependent on π and a more careful analysis of this problem is warranted. We also note that a Moreau-Yosida approximation could be constructed using multiple λ s, and a methodology similar to parallel tempering can be constructed enabling mode-jumping in a multi-modal target. We leave these problems for future work. We also defer the study of asymptotic normality of importance sampling quantiles, as such a result would be applicable even outside the scope of proximal MCMC methods. Finally, we note that since Pereyra (2016), alternative approaches to sampling from non-smooth target densities have been introduced (Lee et al., 2021; Liang and Chen, 2022; Mou et al., 2022). We also leave

the interesting question of how to potentially adapt our importance sampling framework to these contexts for future work.

8 Acknowledgements

Dootika Vats and Eric Chi are grateful to the Rice-IITK Strategic Collaboration Grant for supporting this work. Dootika Vats is also supported by Google Research.

A Proof of Theorem 1

Proof. For normalising constants k_π and k_g , we have

$$\pi(x) = \frac{e^{-\psi(x)}}{k_\pi} \quad \text{and} \quad g(x) = \frac{\tilde{g}(x)}{k_g}.$$

From (2)

$$\hat{\theta}_n^g = \frac{\sum_{t=1}^n \xi(X_t) w(X_t)}{\sum_{k=1}^n w(X_k)} = \frac{n^{-1} \sum_{t=1}^n \xi(X_t) w(X_t)}{n^{-1} \sum_{k=1}^n w(X_k)}.$$

Since $w(x) = e^{-\psi(x)}/\tilde{g}(x)$,

$$\hat{\theta}_n^g = \frac{n^{-1} \sum_{t=1}^n \xi(X_t) \frac{k_\pi \pi(X_t)}{k_g g(X_t)}}{n^{-1} \sum_{k=1}^n \frac{k_\pi \pi(X_k)}{k_g g(X_k)}} =: \frac{Y_n}{Z_n}.$$

By Birkhoff's ergodic theorem (Fristedt and Gray, 1996, Section 28.4), as $n \rightarrow \infty$

$$Y_n = n^{-1} \sum_{t=1}^n \xi(X_t) \frac{k_\pi \pi(X_t)}{k_g g(X_t)} \xrightarrow{\text{a.s.}} \frac{k_\pi}{k_g} \theta,$$

and

$$Z_n = n^{-1} \sum_{k=1}^n \frac{k_\pi \pi(X_k)}{k_g g(X_k)} \xrightarrow{\text{a.s.}} \frac{k_\pi}{k_g}.$$

Therefore, by the continuous mapping theorem $\hat{\theta}_n^g \xrightarrow{\text{a.s.}} \theta$ as $n \rightarrow \infty$. \square

B Proof of Theorem 2

Proof. It is known that given a π^λ -geometrically ergodic Markov chain, a multivariate central limit theorem holds for $\bar{S}_n = n^{-1} \sum_{t=1}^n S(X_t)$ if $\mathbb{E}_{\pi^\lambda} \|S(X)\|^2 < \infty$ (see Kipnis and Varadhan, 1986; Vats, 2017).

Recall that by Durmus et al. (2022), $\psi^\lambda(x) \leq \psi(x)$ for all $x \in \mathbb{R}^d$. Therefore,

$$w^\lambda(x) = \frac{e^{-\psi(x)}}{e^{-\psi^\lambda(x)}} \leq 1,$$

for all $x \in \mathbb{R}^d$ and hence all moments of $w^\lambda(X)$ exist when $X \sim \pi^\lambda$. Further, for constants k_π and k_{π^λ} such that $\pi(x) = e^{-\psi(x)}/k_\pi$ and $\pi^\lambda(x) = e^{-\psi^\lambda(x)}/k_{\pi^\lambda}$, and for all $x \in \mathbb{R}^d$,

$$\sup_{x \in \mathbb{R}^d} \frac{\pi(x)}{\pi^\lambda(x)} = \frac{k_{\pi^\lambda}}{k_\pi} \sup_{x \in \mathbb{R}^d} \frac{e^{-\psi(x)}}{e^{-\psi^\lambda(x)}} \leq \frac{k_{\pi^\lambda}}{k_\pi} < \infty.$$

Given $x \in \mathbb{R}^d$ we write $\xi(x) = (\xi_1(x), \xi_2(x), \dots, \xi_p(x))^\top$, where $\xi_i : \mathbb{R}^d \rightarrow \mathbb{R}$ for all $i = 1, 2, \dots, p$. Thus,

$$\begin{aligned} \mathbb{E}_{\pi^\lambda} |\xi_i(X) w^\lambda(X)|^2 &= \int_{\mathbb{R}^d} |\xi_i(x)|^2 |w^\lambda(x)|^2 \pi^\lambda(x) dx \\ &= \int_{\mathbb{R}^d} |\xi_i(x)|^2 \left(\frac{\exp(-\psi(x))}{\exp(-\psi^\lambda(x))} \right)^2 \pi^\lambda(x) dx \\ &= \left(\frac{k_\pi}{k_{\pi^\lambda}} \right)^2 \int_{\mathbb{R}^d} |\xi_i(x)|^2 \left(\frac{\pi(x)}{\pi^\lambda(x)} \right)^2 \pi^\lambda(x) dx \end{aligned}$$

$$\begin{aligned}
&= \left(\frac{k_\pi}{k_{\pi^\lambda}} \right)^2 \int_{\mathbb{R}^d} |\xi_i(x)|^2 \frac{\pi(x)}{\pi^\lambda(x)} \pi(x) dx \\
&\leq \left(\frac{k_\pi}{k_{\pi^\lambda}} \right)^2 \sup_{x \in \mathbb{R}^d} \frac{\pi(x)}{\pi^\lambda(x)} \int_{\mathbb{R}^d} |\xi_i(x)|^2 \pi(x) dx \\
&\leq \left(\frac{k_\pi}{k_{\pi^\lambda}} \right) \int_{\mathbb{R}^d} |\xi_i(x)|^2 \pi(x) dx \\
&= \left(\frac{k_\pi}{k_{\pi^\lambda}} \right) \mathbb{E}_\pi(|\xi_i(X)|^2).
\end{aligned}$$

Since $\mathbb{E}_\pi \|\xi(X)\|^2 < \infty$, $\mathbb{E}_{\pi^\lambda} |\xi_i(X) w^\lambda(X)|^2$ is finite. Thus, $\mathbb{E}_{\pi^\lambda} \|S(X)\|^2 < \infty$. By a Markov chain central limit theorem, there exists a $(p+1) \times (p+1)$ positive-definite matrix Σ such that,

$$\sqrt{n} (\bar{S}_n - \mathbb{E}_{\pi^\lambda}(S(X))) \xrightarrow{d} N_{p+1}(0, \Sigma), \quad (50)$$

where,

$$\Sigma = \text{Var}_{\pi^\lambda} S(X_1) + \sum_{k=1}^{\infty} \text{Cov}_{\pi^\lambda}(S(X_1), S(X_{1+k})) + \sum_{k=1}^{\infty} \text{Cov}_{\pi^\lambda}(S(X_{1+k}), S(X_1)).$$

Let $\kappa : \mathbb{R}^{p+1} \rightarrow \mathbb{R}^p$ be a continuous real-valued function such that for $u \in \mathbb{R}^p$ and $v \in \mathbb{R}$,

$$\kappa \begin{pmatrix} u \\ v \end{pmatrix} = \frac{u}{v}. \quad (51)$$

Using multivariate delta method in (50) for function κ , as $n \rightarrow \infty$,

$$\sqrt{n} (\kappa(\bar{S}_n) - \kappa(\mathbb{E}_{\pi^\lambda} S(X))) \xrightarrow{d} N_p(0, \nabla \kappa_\eta \Sigma \nabla \kappa_\eta^\top), \quad (52)$$

where $\nabla \kappa_\eta$ is the total derivative of κ at the point $\eta = \mathbb{E}_{\pi^\lambda}[S(X)]$. A sufficient condition for the existence of the total derivative is that all the partial derivatives exist in a neighbourhood of η and are continuous at η (Van der Vaart, 2000). From (51),

writing $u = (u_1, u_2, \dots, u_p)^\top$ where $u_i \in \mathbb{R}$ for all $i = 1, 2, \dots, p$ we have $\kappa(u, v)^\top = (u_1/v, u_2/v, \dots, u_p/v)^\top$. The total derivative is then just the $p \times (p+1)$ matrix of partial derivatives given by

$$\nabla \kappa_{(u,v)^\top} = \begin{bmatrix} \mathbf{I}_p & -\frac{u}{v^2} \end{bmatrix}.$$

Therefore,

$$\begin{aligned} \nabla \kappa_\eta &= \begin{bmatrix} \mathbf{I}_p & -\frac{\mathbb{E}_{\pi^\lambda}(\xi(X)w^\lambda(X))}{(\mathbb{E}_{\pi^\lambda}(w^\lambda(X)))^2} \end{bmatrix} \\ &= \frac{1}{\mathbb{E}_{\pi^\lambda}(w^\lambda(X))} \begin{bmatrix} \mathbf{I}_p & -\theta \end{bmatrix}. \end{aligned}$$

Thus,

$$\nabla \kappa_\eta \Sigma \nabla \kappa_\eta^\top = \frac{1}{(\mathbb{E}_{\pi^\lambda}(w^\lambda(X)))^2} \begin{bmatrix} \mathbf{I}_p & -\theta \end{bmatrix} \Sigma \begin{bmatrix} \mathbf{I}_p \\ -\theta^\top \end{bmatrix} = \Xi. \quad (53)$$

Since $\hat{\theta}_n^{\text{MY}} = \kappa(\bar{S}_n)$ and $\theta = \kappa(\mathbb{E}_{\pi^\lambda} S(X))$, using (53) in (52) we have as $n \rightarrow \infty$,

$$\sqrt{n}(\hat{\theta}_n^{\text{MY}} - \theta) \xrightarrow{d} N_p(0, \Xi).$$

□

C Optimal λ for Gaussian target

Proof of Theorem 4. We first find the form of the MY envelope of ψ for $N(0, \Omega)$ target.

Note that

$$\psi^\lambda(x) = \min_{y \in \mathbb{R}^p} \left\{ \frac{y^\top \Omega^{-1} y}{2} + \frac{(x-y)^\top (x-y)}{2\lambda} \right\}.$$

It is then easy to see that $\text{prox}_\psi^\lambda(x) = (\lambda\Omega^{-1} + \mathbb{I}_d)^{-1}x$. Therefore,

$$\psi^\lambda(x) = \frac{\text{prox}_\psi^\lambda(x)^\top \Omega^{-1} \text{prox}_\psi^\lambda(x)}{2} + \frac{(x - \text{prox}_\psi^\lambda(x))^\top (x - \text{prox}_\psi^\lambda(x))}{2\lambda}. \quad (54)$$

The following two simplifications will be used later

$$\begin{aligned} \frac{\text{prox}_\psi^\lambda(x)^\top \Omega^{-1} \text{prox}_\psi^\lambda(x)}{2} &= \frac{x^\top (\lambda\Omega^{-1} + \mathbb{I}_d)^{-1} \Omega^{-1} (\lambda\Omega^{-1} + \mathbb{I}_d)^{-1} x}{2} \quad \text{and} \\ \frac{(x - \text{prox}_\psi^\lambda(x))^\top (x - \text{prox}_\psi^\lambda(x))}{2\lambda} &= \frac{x^\top (\mathbb{I}_d - (\lambda\Omega^{-1} + \mathbb{I}_d)^{-1})^\top (\mathbb{I}_d - (\lambda\Omega^{-1} + \mathbb{I}_d)^{-1}) x}{2\lambda}. \end{aligned}$$

Using Woodbury identity,

$$(\lambda\Omega^{-1} + \mathbb{I}_d)^{-1} = \mathbb{I}_d - (\mathbb{I}_d + \lambda\Omega^{-1})^{-1} \lambda\Omega^{-1} = \mathbb{I}_d - \lambda\Omega^{-1} (\mathbb{I}_d + \lambda\Omega^{-1})^{-1}.$$

Thus, we obtain

$$\frac{(x - \text{prox}_\psi^\lambda(x))^\top (x - \text{prox}_\psi^\lambda(x))}{2\lambda} = \frac{x^\top (\lambda\Omega^{-1} + \mathbb{I}_d)^{-1} \lambda\Omega^{-1} \Omega^{-1} (\lambda\Omega^{-1} + \mathbb{I}_d)^{-1} x}{2}.$$

So in (54) we have

$$\begin{aligned} \psi^\lambda(x) &= \frac{x^\top (\lambda\Omega^{-1} + \mathbb{I}_d)^{-1} \Omega^{-1} (\lambda\Omega^{-1} + \mathbb{I}_d)^{-1} x}{2} \\ &\quad + \frac{x^\top (\lambda\Omega^{-1} + \mathbb{I}_d)^{-1} \lambda\Omega^{-1} \Omega^{-1} (\lambda\Omega^{-1} + \mathbb{I}_d)^{-1} x}{2} \\ \Rightarrow \psi^\lambda(x) &= \frac{x^\top (\Omega + \lambda\mathbb{I}_d)^{-1} x}{2}. \end{aligned}$$

Since normalizing constants are unique, the MY envelope of $N(0, \Omega)$ is $N(0, (\Omega + \lambda\mathbb{I}_d))$.

Agarwal et al. (2022) provided the form of the asymptotic covariance matrix of the self-normalized importance sampling estimator of $\mathbb{E}_\pi(X)$ when using iid samples from π^λ .

Using their result, we obtain that the limiting covariance matrix for the (iid) self-normalized importance sampling estimator for $\xi(x) = x$ is,

$$\Xi := \frac{|\Omega + \lambda \mathbb{I}_d|^{1/2}}{|\Omega| |2\Omega^{-1} - (\Omega + \lambda \mathbb{I}_d)^{-1}|^{1/2}} (2\Omega^{-1} - (\Omega + \lambda \mathbb{I}_d)^{-1})^{-1}. \quad (55)$$

We may then choose λ based on the value that minimizes $|\Xi|$. The rest of the argument finds this optimal value of λ . First, consider the eigenvalue decomposition of $\Omega = LDL^T$ where L is the orthogonal matrix of the eigenvectors of Ω and $D = \text{diagonal}(s_1, s_2, \dots, s_d)$ where s_i is the i^{th} eigenvalue of Ω . Using this,

$$\begin{aligned} 2\Omega^{-1} - (\Omega + \lambda \mathbb{I}_d)^{-1} &= 2LD^{-1}L - (LDL^T + \lambda LL^T)^{-1} \\ &= L(2D^{-1} - (D + \lambda \mathbb{I}_d)^{-1})L^T \\ &= L \text{diag}(w_1, w_2, \dots, w_p)L^T, \end{aligned} \quad (56)$$

where $w_i = (s_i + 2\lambda)/(s_i(s_i + \lambda))$. Using (56) in (55),

$$\begin{aligned} |\Xi| &= \left| \frac{|\Omega + \lambda \mathbb{I}_d|^{1/2}}{|\Omega| |2\Omega^{-1} - (\Omega + \lambda \mathbb{I}_d)^{-1}|^{1/2}} (2\Omega^{-1} - (\Omega + \lambda \mathbb{I}_d)^{-1})^{-1} \right| \\ &= \left(\frac{|\Omega + \lambda \mathbb{I}_d|^{1/2}}{|\Omega| |2\Omega^{-1} - (\Omega + \lambda \mathbb{I}_d)^{-1}|^{1/2}} \right)^d \left| (2\Omega^{-1} - (\Omega + \lambda \mathbb{I}_d)^{-1})^{-1} \right| \\ \Rightarrow \log |\Xi| &= \frac{d}{2} \log |\Omega + \lambda \mathbb{I}_d| - d \log |\Omega| - \frac{d}{2} \log |2\Omega^{-1} - (\Omega + \lambda \mathbb{I}_d)^{-1}| - \log |2\Omega^{-1} - (\Omega + \lambda \mathbb{I}_d)^{-1}| \\ &= d \sum_{i=1}^d \left[\frac{1}{2} \log(s_i + \lambda) - \log s_i - \frac{1}{2} \log \left(\frac{s_i + 2\lambda}{s_i(s_i + \lambda)} \right) \right] - \sum_{i=1}^d \log \left(\frac{s_i + 2\lambda}{s_i(s_i + \lambda)} \right) \\ &= \sum_{i=1}^d \left((d+1) \log(s_i + \lambda) - \left(\frac{d}{2} - 1 \right) \log s_i - \left(\frac{d}{2} + 1 \right) \log(s_i + 2\lambda) \right) \\ \Rightarrow \frac{d \log |\Xi|}{d\lambda} &= \sum_{i=1}^d \left(\frac{d+1}{s_i + \lambda} - \frac{d+2}{s_i + 2\lambda} \right) \stackrel{\text{set}}{=} 0 \end{aligned}$$

$$\Rightarrow \sum_{i=1}^d \frac{\lambda d - s_i}{(s_i + \lambda)(s_i + 2\lambda)} = 0. \quad (57)$$

We check the existence of a solution to (57) for $\lambda > 0$. Denote $g(\lambda) := \log|\Xi|$, then, $g(\lambda)$ decreases on $[0, s_1/d)$ since $g'(\lambda) < 0$ in this interval. Thus, $g(\lambda) > g(s_1/d)$ for all $\lambda \in [0, s_1/d)$. Similarly $g(\lambda)$ increases on $(s_d/d, \infty)$ since $g'(\lambda) > 0$ on this interval. Thus, $g(\lambda) > g(s_d/d)$ for all $\lambda \in (s_d/d, \infty)$. Since $g(\lambda)$ is continuous, it attains a global minimum over the compact set $[s_1/d, s_d/d]$, i.e., $g(\lambda) \geq g(\lambda^*)$ where $\lambda^* \in [s_1/d, s_d/d]$. But $g(\lambda^*) \leq \min\{g(s_1/d), g(s_d/d)\}$. Therefore, λ^* minimizes $g(\lambda)$ over $\lambda > 0$ and $s_1/d \leq \lambda^* \leq s_d/d$. \square

C.1 Importance sampling ESS in iid Gaussian case

As before, let the target density π be that of $N(0, \Omega)$. Further suppose all the eigenvalues are the same so that $\lambda^* = s_1/d$. Thus, π^{λ^*} is the density of $N(0, W)$, where $W = \Omega + (s_1/d)\mathbb{I}_d$. The importance sampling ESS of Kong (1992) is,

$$\frac{n_e}{n} = \frac{\bar{w}_n^2}{w_n^2} \approx \frac{(\mathbb{E}_{\pi^{\lambda^*}}(w^{\lambda^*}(X)))^2}{\mathbb{E}_{\pi^{\lambda^*}}(w^{\lambda^*}(X)^2)}. \quad (58)$$

Note that,

$$\mathbb{E}_{\pi^{\lambda^*}}(w^{\lambda^*}(X)) = \int_{\mathbb{R}^d} \frac{\pi(x)}{k_{\pi}} \frac{k_{\pi^{\lambda^*}}}{\pi^{\lambda^*}(x)} \pi^{\lambda^*}(x) dx = \frac{k_{\pi}}{k_{\pi^{\lambda^*}}}. \quad (59)$$

Further,

$$\begin{aligned} \mathbb{E}_{\pi^{\lambda^*}}(w^{\lambda^*}(X)^2) &= \int_{\mathbb{R}^d} \frac{\pi(x)^2}{k_{\pi}^2} \frac{k_{\pi^{\lambda^*}}^2}{\pi^{\lambda^*}(x)^2} \pi^{\lambda^*}(x) dx \\ &= \frac{k_{\pi}^2}{k_{\pi^{\lambda^*}}^2} \int_{\mathbb{R}^d} \frac{1}{(\sqrt{2\pi})^d} \frac{|W|^{1/2}}{|\Omega|} \exp(-2\psi(x) + \psi^{\lambda^*}(x)) dx \\ &= \frac{k_{\pi}^2}{k_{\pi^{\lambda^*}}^2} \int_{\mathbb{R}^d} \frac{1}{(\sqrt{2\pi})^d} \frac{|W|^{1/2}}{|\Omega|} \exp\left\{-x^{\top} \Omega^{-1} x + \frac{1}{2} x^{\top} W^{-1} x\right\} dx \end{aligned}$$

$$\begin{aligned}
&= \frac{k_\pi^2}{k_{\pi\lambda}^2} \int_{\mathbb{R}^d} \frac{1}{(\sqrt{2\pi})^d} \frac{|W|^{1/2}}{|\Omega|} \exp \left\{ -\frac{1}{2} \left[x^\top (2\Omega^{-1} - W^{-1}) x \right] \right\} dx \\
&= \frac{k_\pi^2}{k_{\pi\lambda}^2} \frac{|W|^{1/2}}{\Omega} |(2\Omega^{-1} - W^{-1})^{-1}|^{1/2} \times \\
&\quad \int_{\mathbb{R}^d} \frac{1}{(\sqrt{2\pi})^d} \frac{1}{|(2\Omega^{-1} - W^{-1})^{-1}|^{1/2}} \exp \left(-\frac{1}{2} x^\top (2\Omega^{-1} - W^{-1}) x \right) dx.
\end{aligned}$$

It is known that given two conformable matrices A and B , a sufficient condition for $A - B$ to be positive definite is that the minimum eigenvalue of A is greater than the maximum eigenvalue of B . Thus, $(2\Omega^{-1} - W^{-1})$ is positive definite, and the integral on the right hand side in the above equation is 1. Therefore,

$$\mathbb{E}_{\pi^\lambda}(w^\lambda(X)^2) = \frac{k_\pi^2}{k_{\pi\lambda}^2} \frac{|W|^{1/2}}{|\Omega|} |(2\Omega^{-1} - W^{-1})^{-1}|^{1/2}. \quad (60)$$

Using (59) and (60) in (58),

$$\frac{n_e}{n} = \frac{|2\Omega^{-1} - W^{-1}|^{1/2} |\Omega|}{|W|^{1/2}}. \quad (61)$$

Since Ω is a $d \times d$ diagonal matrix with same eigenvalues, namely $\Omega := \text{diag}(s_1)_{d \times d}$,

$$2\Omega^{-1} - W^{-1} = \text{diag} \left(\frac{2}{s_1} - \frac{1}{s_1 + s_1/d} \right) = \text{diag} \left(\frac{1}{s_1} \left(\frac{d+2}{d+1} \right) \right)_{d \times d}.$$

Noting that $|W|^{1/2} = s_1^{d/2} ((d+1)/d)^{d/2}$ and substituting from the last equation into (61)

we have,

$$\frac{n_e}{n} = \frac{(d(d+2))^{d/2}}{(d+1)^d} = \frac{(1+2/d)^{d/2}}{(1+1/d)^d}.$$

Now both numerator and denominator converge to e as $d \rightarrow \infty$. Thus, $n_e/n \rightarrow 1$ as $d \rightarrow \infty$.

D Proofs of geometric ergodicity of π^λ -Markov chains

We will require the following lemma in both the proofs of geometric ergodicity for π^λ -MALA and π^λ -HMC.

Lemma 1. Under Assumption 1,

$$\liminf_{\|x\| \rightarrow \infty} \left\{ \|x\| \left(1 - \frac{\|\text{prox}_\psi^\lambda(x)\|}{\|x\|} \right) \right\} = \infty.$$

Proof. Let $B(t) := \{x : \|x\| > t\}$. Assumption 1 is equivalent to

$$\inf_{t \geq 0} \sup_{x \in B(t)} \frac{\|\text{prox}_\psi^\lambda(x)\|}{\|x\|} = l. \quad (62)$$

Equation (62) implies that for any positive ϵ there exists $t_\epsilon \geq 0$ such that

$$\frac{\|\text{prox}_\psi^\lambda(x)\|}{\|x\|} < l + \epsilon \quad \text{for all } x \in B(t_\epsilon).$$

Consider a sequence $\epsilon_n = 1/n$. Then there exists an increasing and diverging sequence t_n such that

$$\|x\| \left(1 - \frac{\|\text{prox}_\psi^\lambda(x)\|}{\|x\|} \right) > \|x\| \left(1 - l - \frac{1}{n} \right) \quad \text{for all } x \in B(t_n). \quad (63)$$

We will show the existence of such a sequence towards the end of this proof. Taking the infimum of both sides of the inequality (63) over $x \in B(t_n)$,

$$\inf_{x \in B(t_n)} \left\{ \|x\| \left(1 - \frac{\|\text{prox}_\psi^\lambda(x)\|}{\|x\|} \right) \right\} \geq t_n \left(1 - l - \frac{1}{n} \right).$$

Note that for $t \geq t_n$, $B(t) \subset B(t_n)$. Consequently,

$$\inf_{x \in B(t)} \left\{ \|x\| \left(1 - \frac{\|\text{prox}_\psi^\lambda(x)\|}{\|x\|} \right) \right\} \geq t_n \left(1 - l - \frac{1}{n} \right). \quad (64)$$

Taking the limit as $t \rightarrow \infty$ on both sides of the inequality in (64) gives us

$$\liminf_{t \rightarrow \infty} \inf_{x \in B(t)} \left\{ \|x\| \left(1 - \frac{\|\text{prox}_\psi^\lambda(x)\|}{\|x\|} \right) \right\} \geq t_n \left(1 - l - \frac{1}{n} \right). \quad (65)$$

Since t_n is an increasing and diverging sequence, taking the limit as $n \rightarrow \infty$ of both sides of the inequality in (65) gives the desired result.

What is left to show is that there exists an increasing and diverging sequence t_n . Note that there exists \tilde{t}_{n+1} such that

$$\frac{\|\text{prox}_\psi^\lambda(x)\|}{\|x\|} < l + \frac{1}{n+1} \quad \text{for all } x \in B(\tilde{t}_{n+1}).$$

Let $t_{n+1} := \max(\tilde{t}_{n+1}, t_n + 1) \geq t_n + 1 > t_n$. But since $t_{n+1} \geq \tilde{t}_{n+1}$, we have that $B(t_{n+1}) \subset B(\tilde{t}_{n+1})$. Therefore,

$$\frac{\|\text{prox}_\psi^\lambda(x)\|}{\|x\|} < l + \frac{1}{n+1} \quad \text{for all } x \in B(t_{n+1}).$$

□

D.1 Proof of Theorem 6

Proof. We need to show that when $h \leq 2\lambda$

$$\eta := \liminf_{\|x\| \rightarrow \infty} \{\|x\| - \|c(x)\|\} > 0.$$

Recall that $\nabla \log \pi^\lambda(x) = -\lambda^{-1} [x - \text{prox}_\psi^\lambda(x)]$. Therefore,

$$\begin{aligned}
\|x\| - \|c(x)\| &= \|x\| - \left\| x + \frac{h}{2} \nabla \log \pi^\lambda(x) \right\| \\
&= \|x\| - \left\| x - \frac{h}{2\lambda} [x - \text{prox}_\psi^\lambda(x)] \right\| \\
&= \|x\| - \left\| \left(1 - \frac{h}{2\lambda}\right) x + \frac{h}{2\lambda} \text{prox}_\psi^\lambda(x) \right\| \\
&\geq \|x\| - \left| 1 - \frac{h}{2\lambda} \right| \|x\| - \frac{h}{2\lambda} \left\| \text{prox}_\psi^\lambda(x) \right\|,
\end{aligned}$$

where the last inequality follows from the triangle inequality. Since $h/(2\lambda) \leq 1$,

$$\begin{aligned}
\liminf_{\|x\| \rightarrow \infty} \{\|x\| - \|c(x)\|\} &\geq \liminf_{\|x\| \rightarrow \infty} \left\{ \|x\| - \left(1 - \frac{h}{2\lambda}\right) \|x\| - \frac{h}{2\lambda} \left\| \text{prox}_\psi^\lambda(x) \right\| \right\} \\
&= \liminf_{\|x\| \rightarrow \infty} \left\{ \frac{h}{2\lambda} (\|x\| - \left\| \text{prox}_\psi^\lambda(x) \right\|) \right\} \\
&= \frac{h}{2\lambda} \liminf_{\|x\| \rightarrow \infty} \left\{ \|x\| \left(1 - \frac{\left\| \text{prox}_\psi^\lambda(x) \right\|}{\|x\|} \right) \right\} \\
&> 0,
\end{aligned}$$

where the last inequality follows from Lemma 1. □

D.2 Proof of Theorem 9

Proof. We will show that under Assumption 1, conditions (36), (37), and (39) hold, yielding the result. First,

$$\lim_{\|x\| \rightarrow \infty} \|\nabla \psi^\lambda(x)\| = \lim_{\|x\| \rightarrow \infty} \frac{\|x - \text{prox}_\psi^\lambda(x)\|}{\lambda}$$

$$\geq \frac{1}{\lambda} \lim_{\|x\| \rightarrow \infty} \|x\| \left(1 - \frac{\|\text{prox}_{\psi}^{\lambda}(x)\|}{\|x\|} \right) = \infty,$$

using Lemma 1 and the fact that for any sequence a_n , $\liminf a_n \leq \limsup a_n$. Thus, (36) holds.

We move on to showing (37) holds. Let ψ^* denote the Fenchel conjugate of ψ , i.e.,

$$\psi^*(x) = \sup_y \{\langle x, y \rangle - \psi(y)\}.$$

Recall that $\psi^* \in \Gamma(\mathbb{R}^d)$ whenever $\psi \in \Gamma(\mathbb{R}^d)$. Furthermore, recall that if $\psi \in \Gamma(\mathbb{R}^d)$ then by the Moreau decomposition, $x = \text{prox}_{\psi}^{\lambda}(x) + \lambda \text{prox}_{\psi^*}^{1/\lambda}(x/\lambda)$, and thus

$$\nabla \psi^{\lambda}(x) = \frac{1}{\lambda} [x - \text{prox}_{\psi}^{\lambda}(x)] = \text{prox}_{\psi^*}^{1/\lambda}(x/\lambda).$$

Since $\psi^* \in \Gamma(\mathbb{R}^d)$, the proximal mapping is firmly nonexpansive, i.e., for all x and y

$$\|\text{prox}_{\psi^*}^{1/\lambda}(x) - \text{prox}_{\psi^*}^{1/\lambda}(y)\|^2 \leq \langle x - y, \text{prox}_{\psi^*}^{1/\lambda}(x) - \text{prox}_{\psi^*}^{1/\lambda}(y) \rangle. \quad (66)$$

Plugging $(x, y) = (x/\lambda, 0)$ into (66) and rearranging terms gives

$$\begin{aligned} \left\langle \frac{x}{\lambda}, \text{prox}_{\psi^*}^{1/\lambda} \left(\frac{x}{\lambda} \right) \right\rangle &\geq \left\| \text{prox}_{\psi^*}^{1/\lambda} \left(\frac{x}{\lambda} \right) - \text{prox}_{\psi^*}^{1/\lambda}(0) \right\|^2 + \left\langle \frac{x}{\lambda}, \text{prox}_{\psi^*}^{1/\lambda}(0) \right\rangle \\ \Rightarrow \langle x, \nabla \psi^{\lambda}(x) \rangle &\geq \lambda \|\nabla \psi^{\lambda}(x) - \nabla \psi^{\lambda}(0)\|^2 + \langle x, \nabla \psi^{\lambda}(0) \rangle. \end{aligned}$$

Dividing the terms on both sides of the above inequality by $\|x\| \|\nabla \psi^{\lambda}(x)\|$,

$$\begin{aligned} &\frac{\langle x, \nabla \psi^{\lambda}(x) \rangle}{\|x\| \|\nabla \psi^{\lambda}(x)\|} \\ &\geq \lambda \frac{\|\nabla \psi^{\lambda}(x) - \nabla \psi^{\lambda}(0)\|}{\|x\|} \cdot \frac{\|\nabla \psi^{\lambda}(x) - \nabla \psi^{\lambda}(0)\|}{\|\nabla \psi^{\lambda}(x)\|} + \frac{\langle x, \nabla \psi^{\lambda}(0) \rangle}{\|x\| \|\nabla \psi^{\lambda}(x)\|} \end{aligned}$$

$$= \lambda \left[\frac{\|\nabla\psi^\lambda(x)\|}{\|x\|} - \frac{\|\nabla\psi^\lambda(0)\|}{\|x\|} \right] \left[1 - \frac{\|\nabla\psi^\lambda(0)\|}{\|x\|} \right] + \left\langle \frac{x}{\|x\|}, \frac{\nabla\psi^\lambda(0)}{\|\nabla\psi^\lambda(x)\|} \right\rangle. \quad (67)$$

Since $\lim_{\|x\| \rightarrow \infty} \|\nabla\psi^\lambda(x)\| = \infty$,

$$\lim_{\|x\| \rightarrow \infty} \left\langle \frac{x}{\|x\|}, \frac{\nabla\psi^\lambda(0)}{\|\nabla\psi^\lambda(x)\|} \right\rangle = 0. \quad (68)$$

Further, by Assumption 1

$$\begin{aligned} \liminf_{\|x\| \rightarrow \infty} \frac{\|\nabla\psi^\lambda(x)\|}{\|x\|} &= \frac{1}{\lambda} \liminf_{\|x\| \rightarrow \infty} \frac{\|x - \text{prox}_\psi^\lambda(x)\|}{\|x\|} \\ &\geq \frac{1}{\lambda} \liminf_{\|x\| \rightarrow \infty} \left(1 - \frac{\|\text{prox}_\psi^\lambda(x)\|}{\|x\|} \right) \\ &> 0. \end{aligned} \quad (69)$$

Using (68) and (69) in (67),

$$\begin{aligned} &\liminf_{\|x\| \rightarrow \infty} \frac{\langle x, \nabla\psi^\lambda(x) \rangle}{\|x\| \|\nabla\psi^\lambda(x)\|} \\ &\geq \liminf_{\|x\| \rightarrow \infty} \left\{ \lambda \left[\frac{\|\nabla\psi^\lambda(x)\|}{\|x\|} - \frac{\|\nabla\psi^\lambda(0)\|}{\|x\|} \right] \left[1 - \frac{\|\nabla\psi^\lambda(0)\|}{\|x\|} \right] + \left\langle \frac{x}{\|x\|}, \frac{\nabla\psi^\lambda(0)}{\|\nabla\psi^\lambda(x)\|} \right\rangle \right\} \\ &\geq \liminf_{\|x\| \rightarrow \infty} \lambda \left[\frac{\|\nabla\psi^\lambda(x)\|}{\|x\|} - \frac{\|\nabla\psi^\lambda(0)\|}{\|x\|} \right] \left[1 - \frac{\|\nabla\psi^\lambda(0)\|}{\|x\|} \right] + \liminf_{\|x\| \rightarrow \infty} \left\langle \frac{x}{\|x\|}, \frac{\nabla\psi^\lambda(0)}{\|\nabla\psi^\lambda(x)\|} \right\rangle \\ &\geq \liminf_{\|x\| \rightarrow \infty} \lambda \left[\frac{\|\nabla\psi^\lambda(x)\|}{\|x\|} - \frac{\|\nabla\psi^\lambda(0)\|}{\|x\|} \right] \left[1 - \frac{\|\nabla\psi^\lambda(0)\|}{\|x\|} \right] + \liminf_{\|x\| \rightarrow \infty} \left\langle \frac{x}{\|x\|}, \frac{\nabla\psi^\lambda(0)}{\|\nabla\psi^\lambda(x)\|} \right\rangle \\ &\geq \liminf_{\|x\| \rightarrow \infty} \lambda \left[\frac{\|\nabla\psi^\lambda(x)\|}{\|x\|} - \frac{\|\nabla\psi^\lambda(0)\|}{\|x\|} \right] \lim_{\|x\| \rightarrow \infty} \left[1 - \frac{\|\nabla\psi^\lambda(0)\|}{\|x\|} \right] \\ &> 0. \end{aligned}$$

This establishes (37). Next, we show that (39) holds. Note that,

$$\begin{aligned} \frac{\|\nabla\psi^\lambda(x)\|}{\|x\|} &= \frac{1}{\lambda} \frac{\|x - \text{prox}_\psi^\lambda(x)\|}{\|x\|} \\ &\leq \frac{1}{\lambda} \frac{\|x\| + \|\text{prox}_\psi^\lambda(x)\|}{\|x\|} \\ \Rightarrow \limsup_{\|x\| \rightarrow \infty} \frac{\|\nabla\psi^\lambda(x)\|}{\|x\|} &\leq \limsup_{\|x\| \rightarrow \infty} \frac{1}{\lambda} \left(1 + \frac{\|\text{prox}_\psi^\lambda(x)\|}{\|x\|} \right) \leq \frac{2}{\lambda} < \infty. \end{aligned}$$

Thus, $\limsup_{\|x\| \rightarrow \infty} \|\nabla\psi^\lambda(x)\|/\|x\|$ is finite, and (39) holds. By Livingstone et al. (2019), the π^λ -HMC chain is geometrically ergodic for a sufficiently small ϵ . \square

E Details for numerical examples

E.1 Proximal algorithms

The proximal MCMC algorithms used in the examples are the P-MALA and P-HMC algorithms for the trendfiltering and the nuclear norm examples. For the Bayesian Poisson random effects model, Barker’s algorithm is implemented and compared with the proximal versions.

The primary features of the proximal adaptations of the MALA and HMC are the following.

1. Use the gradient of the approximated target π^λ , i.e. $\nabla \log \pi^\lambda(x)$ in the proposal step.
2. Maintain π -invariance of the algorithm by employing the Metropolis-Hastings correction step with respect to π .

Thus, although the proximal MCMC algorithms use the gradient information of the smooth approximations to the target density, they employ the M-H correction step to maintain π

invariance resulting in samples from π . The algorithms for proposing samples using P-MALA and P-HMC are given below.

Algorithm 3 P-MALA for π given $h > 0$

1. Given $X_t = x$, generate proposal $(Y = y) \sim q_M(x, \cdot) \equiv N\left(x - \frac{h}{2}\nabla\psi^\lambda(x), h\mathbb{I}_d\right)$
2. Generate $U \sim U(0, 1)$ independently and set

$$\alpha(x, y) = \min\left\{1, \frac{\pi(y)q_M(y, x)}{\pi(x)q_M(x, y)}\right\}$$

3. If $U \leq \alpha(x, y)$, then $X_{t+1} = y$
 4. Else $X_{t+1} = x$
-

The Barker's algorithm due to Livingstone and Zanella (2022) uses the gradients of the target in the proposal density,

$$q_B(x, y) = 2 \cdot \frac{q_h(y - x)}{1 + e^{-(y-x)^\top \nabla \log \pi(x)}} \quad (70)$$

where $q_h(\cdot)$ denotes the Gaussian density with variance h . Algorithms 5 and 6 give a straightforward way to propose from (70).

E.2 Bayesian trendfiltering

The MY envelope of $\psi(\mu)$ is given by

$$\begin{aligned} \psi^\lambda(\mu) &= \min_{\eta \in \mathbb{R}^d} \left\{ \psi(\eta) + \frac{1}{2\lambda} \|\mu - \eta\|_2^2 \right\} \\ &= \min_{\eta \in \mathbb{R}^d} \left\{ \frac{\|y - \eta\|_2^2}{2\sigma^2} + \frac{1}{2\lambda} \|\mu - \eta\|_2^2 + \alpha \left\| \mathbf{D}_m^{(k+1)} \eta \right\|_1 \right\}, \end{aligned}$$

Algorithm 4 P-HMC for π given $\varepsilon > 0$, L a positive integer and M a p.d. matrix

1. Given $X_t = x$, $\varepsilon > 0$, and $L \geq 1$
2. Set $x_0 = x$, draw $z_0 \sim N(0, M)$
3. Use the *leapfrog* one- ε step equations

$$\begin{aligned}z_{\frac{\varepsilon}{2}} &= z_0 - \frac{\varepsilon}{2} \nabla \psi^\lambda(x_0) \\x_\varepsilon &= x_0 + \varepsilon M^{-1} z_{\frac{\varepsilon}{2}} \\z_\varepsilon &= z_{\frac{\varepsilon}{2}} - \frac{\varepsilon}{2} \nabla \psi^\lambda(x_\varepsilon)\end{aligned}$$

L times sequentially to reach $(x_0, z_0) \rightarrow (x_{L\varepsilon}, z_{L\varepsilon})$

4. Draw $U \sim U(0, 1)$ and calculate,

$$\alpha(x_0, x_{L\varepsilon}) = \min \left\{ 1, e^{-H(x_{L\varepsilon}, z_{L\varepsilon}) + H(x_0, z_0)} \right\}$$

where $H(x, z) = \psi(x) + \frac{1}{2} z^T M^{-1} z$ denotes total energy at (x, z)

5. If $U \leq \alpha(x_0, x_{L\varepsilon})$, then $X_{t+1} = x_{L\varepsilon}$
 6. Else $X_{t+1} = x$
-

Algorithm 5 Barker proposal on \mathbb{R}^d

1. Draw $z \sim q_h(\cdot)$
 2. Calculate $\phi(x, z) = 1/(1 + e^{-z^T \nabla \log \pi^\lambda(x)})$
 3. Set $b(x, z) = 1$ with probability $\phi(x, z)$, and $b(x, z) = -1$ otherwise
 4. Set $y = x + b(x, z) \times z$
-

Algorithm 6 Metropolis-Hastings with Barker's proposal

1. Given $X_t = x$, generate proposal $(Y = y) \sim q_B(x, \cdot)$ using Algorithm 5
2. Generate $U \sim U(0, 1)$ independently and set

$$\alpha(x, y) = \left\{ 1, \frac{\pi(y) q_B(y, x)}{\pi(x) q_B(x, y)} \right\}$$

3. If $U \leq \alpha(x, y)$, then $X_{t+1} = y$
 4. Else $X_{t+1} = x$
-

or equivalently,

$$\psi^\lambda(\mu) = \frac{\|y - \text{prox}_\psi^\lambda(\mu)\|_2^2}{2\sigma^2} + \frac{1}{2\lambda} \|\mu - \text{prox}_\psi^\lambda(\mu)\|_2^2 + \alpha \left\| \mathbf{D}_m^{(k+1)} \text{prox}_\psi^\lambda(\mu) \right\|_1,$$

where

$$\text{prox}_\psi^\lambda(\mu) = \arg \min_{\eta \in \mathbb{R}^d} \left\{ \frac{\|y - \eta\|_2^2}{2\sigma^2} + \frac{1}{2\lambda} \|\mu - \eta\|_2^2 + \alpha \|\mathbf{D}_m^{(k+1)} \eta\|_1 \right\}. \quad (71)$$

Completing the square of the quadratic terms in the expression within the braces of (71) enables us to express the proximal mapping of ψ as

$$\text{prox}_\psi^\lambda(\mu) = \arg \min_{\eta \in \mathbb{R}^d} \left\{ \frac{1}{2} \|\eta - z\|_2^2 + \frac{\alpha \sigma^2 \lambda}{\sigma^2 + \lambda} \|\mathbf{D}_m^{(k+1)} \eta\|_1 \right\}, \quad (72)$$

where

$$z = \frac{\sigma^2}{\sigma^2 + \lambda} \mu + \frac{\lambda}{\sigma^2 + \lambda} y.$$

The optimization problem in (72) is solved by an ADMM algorithm implemented in the `trendfilter` function of the `glmgen` R package available at <https://github.com/statsmaths/glmgen>.

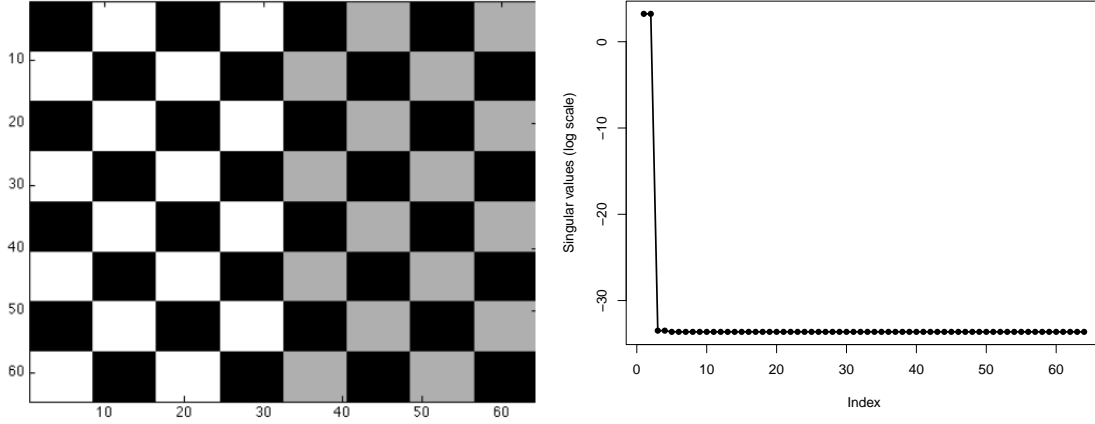


Figure 11: Checkerboard image (*left*), singular values (*right*).

E.3 Nuclear-norm based low rank matrix estimation

We consider the 64×64 checkerboard image of MATLAB, shown in the left panel of Figure 11. The image is low rank as seen in the plot of the singular values of the SVD of the image shown in the right panel of Figure 11.

E.4 MY envelope for Bayesian Poisson random effects

We first derive the joint posterior density function of the Poisson random effects model. The joint prior of η_i 's and μ is given by,

$$\begin{aligned}
 p(\eta_1, \eta_2, \dots, \eta_I, \mu) &= f(\mu) \prod_{i=1}^I f(\eta_i | \mu) \\
 &\propto \exp\left(-\frac{\mu^2}{2c^2}\right) \prod_{i=1}^I \exp\left(-\frac{1}{2\sigma_\eta^2}(\eta_i - \mu)^2\right) \\
 &\propto \exp\left(-\frac{\sum_{i=1}^I (\eta_i^2 + \mu^2 - 2\eta_i \mu)}{2\sigma_\eta^2}\right) \exp\left(-\frac{\mu^2}{2c^2}\right)
 \end{aligned}$$

$$\begin{aligned}
&\propto \exp \left[- \left(\frac{\sum_{i=1}^I \eta_i^2}{2\sigma_\eta^2} + \frac{\mu^2 I}{2\sigma_\eta^2} - \frac{\mu \sum_{i=1}^I \eta_i}{\sigma_\eta^2} \right) \right] \exp \left[-\frac{\mu^2}{2c^2} \right] \\
&\propto \exp \left[- \left(\frac{\sum_{i=1}^I \eta_i^2}{2\sigma_\eta^2} + \frac{\mu^2}{2} \left(\frac{I}{\sigma_\eta^2} + \frac{1}{c^2} \right) - \frac{\mu \sum_{i=1}^I \eta_i}{\sigma_\eta^2} \right) \right]. \quad (73)
\end{aligned}$$

Further, the likelihood function of the observed data is,

$$\begin{aligned}
L(\eta_1, \eta_2, \dots, \eta_I, \mu | y) &= \prod_{i=1}^I \prod_{j=1}^{n_i} \frac{\exp(-e^{\eta_i}) \cdot e^{\eta_i y_{ij}}}{y_{ij}!} \\
&= \prod_{i=1}^I \prod_{j=1}^{n_i} \frac{\exp(\eta_i y_{ij} - e^{\eta_i})}{y_{ij}!} \\
&= \frac{\exp(\sum_{i=1}^I \sum_{j=1}^{n_i} (\eta_i y_{ij} - e^{\eta_i}))}{\prod_{i=1}^I \prod_{j=1}^{n_i} y_{ij}!} \\
&= \frac{\exp(\sum_{i=1}^I (\eta_i \sum_{j=1}^{n_i} y_{ij}) - \sum_{i=1}^I n_i e^{\eta_i})}{\prod_{i=1}^I \prod_{j=1}^{n_i} y_{ij}!}. \quad (74)
\end{aligned}$$

Combining the prior (73) and likelihood (74) gives us the posterior

$$p(\eta_1, \eta_2, \dots, \eta_I, \mu | y) \propto \exp(-\psi(\eta_1, \eta_2, \dots, \eta_I, \mu)),$$

where

$$\psi(\eta_1, \eta_2, \dots, \eta_I, \mu) = \frac{\sum_{i=1}^I \eta_i^2}{2\sigma_\eta^2} - \frac{\mu \sum_{i=1}^I \eta_i}{\sigma_\eta^2} + \sum_{i=1}^I n_i e^{\eta_i} - \sum_{i=1}^I \left(\eta_i \sum_{j=1}^{n_i} y_{ij} \right) + \frac{\mu^2}{2} \left(\frac{I}{\sigma_\eta^2} + \frac{1}{c^2} \right).$$

The proximal mapping for ψ does not admit a closed form solution, so we resort to an iterative algorithm using a Newton-Raphson method. This requires evaluating the gradient $\nabla\psi$ and Hessian $\nabla^2\psi$. Denote $u := (\eta_1, \eta_2, \dots, \eta_I, \mu)$. Then,

$$\psi'_{\eta_i}(u) := \frac{\partial\psi(u)}{\partial\eta_i} = \frac{\eta_i}{\sigma_\eta^2} - \frac{\mu}{\sigma_\eta^2} + n_i e^{\eta_i} - \sum_{j=1}^{n_i} y_{ij}$$

for $i = 1, 2, 3, \dots, I$, and,

$$\psi'_\mu(u) := \frac{\partial \psi(u)}{\partial \mu} = \mu \left(\frac{I}{\sigma_\eta^2} + \frac{1}{c^2} \right) - \frac{\sum_{i=1}^I \eta_i}{\sigma_\eta^2}.$$

Thus, the $(I + 1) \times 1$ first order derivative $\nabla \psi(u)$ can be written as,

$$\nabla \psi(u) = (-\psi_{\eta_1}(u), -\psi_{\eta_2}(u), \dots, -\psi_{\eta_I}(u), -\psi_\mu(u))^\top. \quad (75)$$

Since for a given u ,

$$\text{prox}_\psi^\lambda(u) = \arg \min_{v \in \mathbb{R}^{I+1}} \left\{ \psi(v) + \frac{\|u - v\|^2}{2\lambda} \right\} =: \arg \min_{v \in \mathbb{R}^{I+1}} f_u^\lambda(v),$$

the proximal mapping is the solution of,

$$\nabla f_u^\lambda(v) = \nabla \psi(v) - \frac{u - v}{\lambda} \stackrel{\text{set}}{=} 0. \quad (76)$$

Using (75) in (76), we get the proximal solution $\tilde{v} = (\tilde{\eta}_1, \tilde{\eta}_1, \dots, \tilde{\eta}_I, \tilde{\mu})$. In particular,

$$\tilde{\mu} = \frac{\sum_{i=1}^I \eta_i / \sigma_\eta^2 + \mu / \lambda}{(I / \sigma_\eta^2 + 1 / c^2 + 1 / \lambda)}.$$

Evaluating \tilde{v} is difficult analytically so we apply the Newton-Raphson algorithm. We require the Hessian of f_u^λ with respect to (η_1, \dots, η_I) i.e.,

$$\nabla_\eta^2 f_u^\lambda(v) := \text{diag}(k_{11}, k_{22}, \dots, k_{II}),$$

where $k_{ii} = 1/\sigma_\eta^2 + n_i e^{\eta_i} + 1/\lambda$, and ∇_η^2 is a map from $\mathbb{R}^{(I+1) \times 1} \rightarrow \mathbb{R}^{I \times I}$. Let $\eta^k = (\eta_1^k, \eta_2^k, \dots, \eta_I^k)$ be the vector of η_i 's at the k^{th} step. Then the one step Newton-Raphson algorithm to generate $v^{k+1} = (\eta^{k+1}, \mu^{k+1})^\top$ given $v^k = (\eta^k, \mu^k)^\top$ is given in algorithm 7.

The algorithm stops when,

$$\|\nabla f_u^\lambda(v^*)\| < \epsilon$$

for a specified tolerance ϵ and v^* is the approximate minimizer.

Algorithm 7 Newton-Raphson

- 1: Initialize $v^0 = (\eta^0, \mu^0)^\top$
 - 2: $k \leftarrow 0$
 - 3: **repeat**
 - 4: $\eta^{k+1} = \eta^k - \{\nabla_\eta^2 f_u^\lambda(v^k)\}^{-1} \nabla_\eta f_u^\lambda(v^k)$
 - 5: $\mu^{k+1} = \frac{\sum_{i=1}^I \eta_i^{k+1} / \sigma_\eta^2 + \mu / \lambda}{(I / \sigma_\eta^2 + 1 / c^2 + 1 / \lambda)}$
 - 6: $v^{k+1} = (\eta^{k+1}, \mu^{k+1})^\top$
 - 7: $k \leftarrow k + 1$
 - 8: **until** $\|\nabla f_u^\lambda(v^k)\| < \epsilon$
-

References

- Agarwal, M., Vats, D., and Elvira, V. (2022). A principled stopping rule for importance sampling. *Electronic Journal of Statistics*, 16(2):5570–5590.
- Banerjee, A. and Vats, D. (2024). Efficient multivariate initial sequence estimators for MCMC. *arXiv preprint arXiv:2406.15874*.
- Berg, S. and Song, H. (2023). Efficient shape-constrained inference for the autocovariance sequence from a reversible Markov chain. *The Annals of Statistics*, 51(6):2440–2470.
- Beskos, A., Pillai, N. S., Roberts, G. O., Sanz-Serna, J., and Stuart, A. (2013). Optimal tuning of the hybrid Monte Carlo algorithm. *Bernoulli*, 19(5a):1501–1534.
- Betancourt, M., Byrne, S., Livingstone, S., and Girolami, M. (2017). The geometric foundations of Hamiltonian Monte Carlo. *Bernoulli*, 23(4A):2257–2298.
- Buta, E. and Doss, H. (2011). Computational approaches for empirical Bayes methods and bayesian sensitivity analysis. *The Annals of Statistics*, pages 2658–2685.
- Cai, J.-F., Candès, E. J., and Shen, Z. (2010). A singular value thresholding algorithm for matrix completion. *SIAM Journal on Optimization*, 20(4):1956–1982.

- Chaari, L., Tourneret, J.-Y., Chaux, C., and Batatia, H. (2016). A Hamiltonian Monte Carlo method for non-smooth energy sampling. *IEEE Transactions on Signal Processing*, 64(21):5585–5594.
- Chen, D.-F. R. and Seila, A. F. (1987). Multivariate inference in stationary simulation using batch means. In *Proceedings of the 19th Conference on Winter simulation*, pages 302–304. ACM.
- Chen, M.-H. and Shao, Q.-M. (1999). Monte Carlo estimation of Bayesian credible and HPD intervals. *Journal of Computational and Graphical Statistics*, pages 69–92.
- Combettes, P. L. and Pesquet, J.-C. (2011). *Proximal Splitting Methods in Signal Processing*, pages 185–212. Springer New York, New York, NY.
- Combettes, P. L. and Wajs, V. R. (2005). Signal recovery by proximal forward-backward splitting. *Multiscale Modeling & Simulation*, 4(4):1168–1200.
- Dai, N. and Jones, G. L. (2017). Multivariate initial sequence estimators in Markov chain Monte Carlo. *Journal of Multivariate Analysis*, 159:184–199.
- Durmus, A., Moulines, É., and Pereyra, M. (2022). A proximal Markov chain Monte Carlo method for Bayesian inference in imaging inverse problems: When Langevin meets Moreau. *SIAM Review*, 64(4):991–1028.
- Elvira, V., Chouzenoux, É., and Akyildiz, O. D. (2024). A proximal newton adaptive importance sampler. *arXiv preprint arXiv:2412.16558*.
- Faulkner, J. R. and Minin, V. N. (2018). Locally adaptive smoothing with Markov random fields and shrinkage priors. *Bayesian Analysis*, 13(1):225.
- Fazel, M. (2002). *Matrix rank minimization with applications*. PhD thesis, Stanford University.
- Flegel, J. M. and Kurtz-Garcia, R. P. (2024). Implementing MCMC: Multivariate estimation with confidence. *arXiv preprint arXiv:2408.15396*.
- Fristedt, B. and Gray, L. (1996). *A Modern Approach to Probability Theory*. Probability and Its Applications. Birkhäuser Boston.
- Geyer, C. J. (1992). Practical Markov chain Monte Carlo. *Statistical Science*, pages 473–483.
- Girolami, M. and Calderhead, B. (2011). Riemann manifold Langevin and Hamiltonian Monte Carlo methods. *Journal of the Royal Statistical Society Series B: Statistical Methodology*, 73(2):123–214.

- Glynn, P. W. et al. (1996). Importance sampling for Monte Carlo estimation of quantiles. In *Mathematical Methods in Stochastic Simulation and Experimental Design: Proceedings of the 2nd St. Petersburg Workshop on Simulation*, pages 180–185. Citeseer.
- Glynn, P. W. and Whitt, W. (1991). Estimating the asymptotic variance with batch means. *Operations Research Letters*, 10:431–435.
- Heng, Q., Zhou, H., and Chi, E. C. (2023). Bayesian trend filtering via proximal Markov chain Monte Carlo. *Journal of Computational and Graphical Statistics*, 32(3):938–949.
- Hesterberg, T. C. (1988). *Advances in importance sampling*. Stanford University.
- Hu, W., Shen, W., Zhou, H., and Kong, D. (2020). Matrix linear discriminant analysis. *Technometrics*, 62(2):196–205.
- Jones, G. L. (2004). On the Markov chain central limit theorem. *Probability Surveys*, 1:299–320.
- Kim, S.-J., Koh, K., Boyd, S., and Gorinevsky, D. (2009). ℓ_1 trend filtering. *SIAM Review*, 51(2):339–360.
- Kipnis, C. and Varadhan, S. R. S. (1986). Central limit theorem for additive functionals of reversible Markov processes and applications to simple exclusions. *Comm. Math. Phys.*, 104(1):1–19.
- Kloek, T. and Van Dijk, H. K. (1978). Bayesian estimates of equation system parameters: an application of integration by Monte Carlo. *Econometrica: Journal of the Econometric Society*, pages 1–19.
- Kong, A. (1992). A note on importance sampling using standardized weights. *University of Chicago, Dept. of Statistics, Tech. Rep.*, 348:14.
- Kowal, D. R., Matteson, D. S., and Ruppert, D. (2019). Dynamic shrinkage processes. *Journal of the Royal Statistical Society Series B: Statistical Methodology*, 81(4):781–804.
- Lee, Y. T., Shen, R., and Tian, K. (2021). Structured logconcave sampling with a restricted gaussian oracle. In Belkin, M. and Kpotufe, S., editors, *Proceedings of Thirty Fourth Conference on Learning Theory*, volume 134 of *Proceedings of Machine Learning Research*, pages 2993–3050.
- Liang, J. and Chen, Y. (2022). A proximal algorithm for sampling from non-smooth potentials. In *2022 Winter Simulation Conference (WSC)*, pages 3229–3240.
- Liesenfeld, R. and Richard, J.-F. (2008). Improving MCMC, using efficient importance sampling. *Computational Statistics & Data Analysis*, 53(2):272–288.

- Livingstone, S., Betancourt, M., Byrne, S., and Girolami, M. (2019). On the geometric ergodicity of Hamiltonian Monte Carlo. *Bernoulli*, 25(4A):3109–3138.
- Livingstone, S. and Zanella, G. (2022). The Barker proposal: Combining robustness and efficiency in gradient-based MCMC. *Journal of the Royal Statistical Society Series B: Statistical Methodology*, 84(2):496–523.
- Llorente, F., Curbelo, E., Martino, L., Elvira, V., and Delgado, D. (2022). MCMC-driven importance samplers. *Applied Mathematical Modelling*, 111:310–331.
- Madras, N. and Piccioni, M. (1999). Importance sampling for families of distributions. *Ann. Appl. Probab.*, 9(4):1202–1225.
- Martino, L., Elvira, V., and Camps-Valls, G. (2018). Group importance sampling for particle filtering and MCMC. *Digital Signal Processing*, 82:133–151.
- Mazumder, R., Hastie, T., and Tibshirani, R. (2010). Spectral regularization algorithms for learning large incomplete matrices. *Journal of Machine Learning Research*, 11(80):2287–2322.
- Meyn, S. P. and Tweedie, R. L. (2012). *Markov Chains and Stochastic Stability*. Springer Science & Business Media.
- Mou, W., Flammarion, N., Wainwright, M. J., and Bartlett, P. L. (2022). An efficient sampling algorithm for non-smooth composite potentials. *Journal of Machine Learning Research*, 23(233):1–50.
- Neal, R. M. (2011). MCMC using Hamiltonian dynamics. In *Handbook of Markov chain Monte Carlo*, Chapman & Hall/CRC Handb. Mod. Stat. Methods, pages 113–162. CRC Press, Boca Raton, FL.
- Neal, R. M. et al. (2011). MCMC using Hamiltonian dynamics. *Handbook of Markov chain Monte Carlo*, 2(11):2.
- Osmundsen, K. K., Kleppe, T. S., and Liesenfeld, R. (2021). Importance sampling-based transport map Hamiltonian Monte Carlo for Bayesian hierarchical models. *J. Comput. Graph. Statist.*, 30(4):906–919.
- Parikh, N., Boyd, S., et al. (2014). Proximal algorithms. *Foundations and trends® in Optimization*, 1(3):127–239.
- Pereyra, M. (2016). Proximal Markov chain Monte Carlo algorithms. *Statistics and Computing*, 26:745–760.
- Polson, N. G., Scott, J. G., and Willard, B. T. (2015). Proximal algorithms in statistics and machine learning. *Statistical Science*, 30(4):559–581.

- Recht, B., Fazel, M., and Parrilo, P. A. (2010). Guaranteed minimum-rank solutions of linear matrix equations via nuclear norm minimization. *SIAM review*, 52(3):471–501.
- Richard, J.-F. and Zhang, W. (2007). Efficient high-dimensional importance sampling. *Journal of Econometrics*, 141(2):1385–1411.
- Roberts, G. O. and Rosenthal, J. S. (1998). Optimal scaling of discrete approximations to Langevin diffusions. *Journal of the Royal Statistical Society: Series B (Statistical Methodology)*, 60(1):255–268.
- Roberts, G. O. and Rosenthal, J. S. (2001). Markov chains and de-initializing processes. *Scandinavian Journal of Statistics*, 28:489–504.
- Roberts, G. O. and Sahu, S. K. (1997). Updating schemes, correlation structure, blocking and parameterization for the gibbs sampler. *Journal of the Royal Statistical Society Series B: Statistical Methodology*, 59(2):291–317.
- Roberts, G. O. and Tweedie, R. L. (1996). Exponential convergence of Langevin distributions and their discrete approximations. *Bernoulli*, pages 341–363.
- Roualdes, E. A. (2015). Bayesian trend filtering. *arXiv preprint arXiv:1505.07710*.
- Roy, V. (2019). Convergence diagnostics for Markov chain Monte Carlo. *Annual Review of Statistics and Its Application*, 7.
- Schuster, I. and Klebanov, I. (2020). Markov chain importance sampling—a highly efficient estimator for MCMC. *Journal of Computational and Graphical Statistics*, 30(2):260–268.
- Seila, A. F. (1982). Multivariate estimation in regenerative simulation. *Operations Research Letters*, 1:153–156.
- Silva, L. A. and Zanella, G. (2023). Robust leave-one-out cross-validation for high-dimensional Bayesian models. *Journal of the American Statistical Association*, pages 1–13.
- Song, H. and Berg, S. (2024). Multivariate moment least-squares variance estimators for reversible markov chains. *Journal of Computational and Graphical Statistics*, to appear.
- Tan, A., Doss, H., and Hobert, J. P. (2015). Honest importance sampling with multiple markov chains. *Journal of Computational and Graphical Statistics*, 24(3):792–826.
- Tibshirani, R., Saunders, M., Rosset, S., Zhu, J., and Knight, K. (2005). Sparsity and smoothness via the fused lasso. *Journal of the Royal Statistical Society Series B: Statistical Methodology*, 67(1):91–108.

- Tierney, L. (1994). Markov chains for exploring posterior distributions (with discussion). *The Annals of Statistics*, 22:1701–1762.
- Van der Vaart, A. W. (2000). *Asymptotic Statistics*, volume 3. Cambridge University Press.
- Vats, D. (2017). *Output Analysis for Markov Chain Monte Carlo*. PhD thesis, University of Minnesota.
- Vats, D. and Flegal, J. M. (2022). Lugsail lag windows for estimating time-average covariance matrices. *Biometrika*, 109(3):735–750.
- Vats, D., Flegal, J. M., and Jones, G. L. (2018). Strong consistency of multivariate spectral variance estimators in Markov chain Monte Carlo. *Bernoulli*, 24:1860–1909.
- Vats, D., Flegal, J. M., and Jones, G. L. (2019). Multivariate output analysis for Markov chain Monte Carlo. *Biometrika*, 106(2):321–337.
- Vogrinc, J., Livingstone, S., and Zanella, G. (2023). Optimal design of the Barker proposal and other locally balanced Metropolis–Hastings algorithms. *Biometrika*, 110(3):579–595.
- Zhou, H. and Li, L. (2013). Regularized matrix regression. *Journal of the Royal Statistical Society Series B: Statistical Methodology*, 76(2):463–483.